

SUPPORTING INFORMATION:

Headgroup Structure and Cation Binding in Phosphatidylserine Lipid Bilayers

Hanne Antila,[†] Pavel Buslaev,[‡] Fernando Favela-Rosales,[¶] Tiago M. Ferreira,[§]
Ivan Gushchin,[‡] Matti Javanainen,^{||} Batuhan Kav,[†] Jesper J. Madsen,[⊥] Josef
Melcr,^{||,⑧} Markus S. Miettinen,[†] Jukka Määttä,[△] Ricky Nencini,^{||} O. H. Samuli
Ollila,^{*,||} and Thomas J. Piggot^{††}

*Department of Theory and Bio-Systems, Max Planck Institute of Colloids and Interfaces,
14424 Potsdam, Germany, Research Center for Molecular Mechanisms of Aging and
Age-Related Diseases, Moscow Institute of Physics and Technology, Dolgoprudny 141701,
Russia, Departamento de Investigación, Tecnológico Nacional de México Campus Zacatecas
Occidente, C. P. 99102, Zacatecas, México, NMR Group - Institute for Physics,
Martin-Luther University Halle-Wittenberg, 06120 Halle (Saale), Germany, Institute of
Organic Chemistry and Biochemistry of the Czech Academy of Sciences, Flemingovo nám.
542/2, CZ-16610 Prague 6, Czech Republic, Department of Chemistry, The University of
Chicago, 60637 Chicago, Illinois, United States of America, Department of Global Health,
College of Public Health, University of South Florida, 33612 Tampa, Florida, United States
of America, Groningen Biomolecular Sciences and Biotechnology Institute and The Zernike
Institute for Advanced Materials, University of Groningen, 9747 AG Groningen, The
Netherlands, Department of Chemistry and Materials Science, Aalto University, 00076 Aalto,
Finland, Institute of Biotechnology, University of Helsinki, 00014 Helsinki, Finland, and
Chemistry, University of Southampton, Highfield, Southampton SO17 1BJ, U.K*

E-mail: samuli.ollila@helsinki.fi

S1 Simulated systems

S1.1 CHARMM36

POPC bilayer. Previously published values¹ calculated from the data available from Ref. 2 are used.

DOPS and POPS bilayers. Starting structures were constructed using the CHARMM-GUI webserver.^{3,4} The systems contained a total of 128 lipids (64 per leaflet of the membrane), 35 waters per lipid, and 128 Na⁺ ions. Force field parameters for DOPS and POPS were taken from Venable et al. and included the modified parameters for interactions with Na⁺ ions.⁵ Water was treated using the CHARMM TIP3P model.^{6,7} For POPS, an identical system was also constructed, in which the 128 Na⁺ ions were replaced with 128 K⁺ ions.

Simulations of these systems were performed for 500 ns using GROMACS, version 5.0.6.⁸ A 2 fs timestep was applied during the simulations, and the LINCS algorithm was used to constrain all bonds to hydrogen atoms.^{9,10} For each of the DOPS and POPS systems, two simulations were performed using different randomly assigned starting velocities. The simulations were maintained at temperatures of 303 K for DOPS and 298 K for POPS using the Nosé–Hoover thermostat^{11,12} with a coupling constant of 1 ps. A pressure of 1 bar was maintained using the Parrinello–Rahman¹³ method with a coupling constant of 5 ps. Pressure coupling was applied in a semi-isotropic manner with the *x* and *y* dimensions, in the plane of the bilayer, fluctuating independently of the *z* dimension. Standard CHARMM36 force field methods were used for the simulation cut-offs: van der Waals interactions were truncated at

*To whom correspondence should be addressed

[†]Max Planck Institute of Colloids and Interfaces

[‡]Moscow Institute of Physics and Technology

[¶]Tecnológico Nacional de México

[§]Martin-Luther University Halle-Wittenberg

^{||}Czech Academy of Sciences

[⊥]University of Chicago

[#]University of South Florida

[@]University of Groningen

[△]Aalto University

[▽]University of Helsinki

^{††}University of Southampton

1.2 nm with the interactions switched off between 1.0 nm and 1.2 nm; Coulombic interactions were truncated at 1.2 nm with long-range interactions treated using PME.^{14,15} The final 100 ns of the simulations was used for analysis.

POPC:POPS mixtures without additional ions. Inputs for simulations of POPC:POPS (5:1) mixtures containing a total of 132 lipids (110 POPC and 22 POPS) were created using the CHARMM-GUI.^{3,4} Two identical systems were constructed, apart from the counter ion; one system was neutralised through the addition of 22 Na⁺ ions while the other system contained 22 K⁺ ions. As in the pure POPS CHARMM36 simulations, 35 waters per lipid were added. All other system and simulation parameters and settings were identical to those used in the CHARMM36 POPS simulations.

Simulations of POPC:POPS (5:1) and POPC:POPS (1:1) mixtures containing a total of 300 lipids (250:50 and 150:150) with neutralizing potassium counterions were prepared using the CHARMM-GUI.^{3,4} The systems were simulated using Gromacs 5⁸ and the CHARMM36 force field with simulation parameters given by the CHARMM-GUI at 298 K. For further details see Table S1.

POPC:POPS (5:1) mixtures with additional monovalent ions. POPC:POPS (110:22) mixtures containing a total of 132 lipids, with additional potassium or sodium ions corresponding to concentrations of ~450 mM and 890 mM were generated with the CHARMM-GUI.^{3,4} Systems were simulated using Gromacs 5⁸ and the CHARMM36 force field with simulation parameters given by the CHARMM-GUI at 298 K. For further details, simulation files and data, see Table S1 and Refs. 20,21,23,24.

POPC:POPS (5:1) mixtures with additional calcium using the NBfix1 parameters. POPC:POPS (5:1) mixtures containing a total of 300 (250:50) lipids and 0.26 M and 1 M CaCl₂ were prepared using the CHARMM-GUI in January 2018.^{3,4} The ion parameters generated by the CHARMM-GUI at the time are labeled here as NBfix1.³⁸ Systems were simulated using Gromacs 5⁸ and the CHARMM36 force field with simulation parameters given by the CHARMM-GUI at 298 K.

Table S1: POPC:POPS mixtures simulated with different amounts of added monovalent ions. Salt concentrations are calculated as $[\text{salt}] = N_c \times [\text{water}] / N_w$, where $[\text{water}] = 55.5 \text{ M}$. This corresponds to the concentration in buffer before solvating lipids, as reported in the experiments by Roux et al.^{1,6}

lipids/counter-ion	force field for lipids / ion	^a C _{ci} (M)	^b N ₁	^c N _w	^d N _c	^e T (K)	^f t _{sim} (ns)	^g t _{anal} (ns)	^h files
POPC:POPS (5:1)/K ⁺	CHARMM36 ^{5,17}	0	250:50	11207	0	298	200	180	18
POPC:POPS (5:1)/K ⁺	CHARMM36 ^{5,17}	0	110:22	4620	0	298	500	100	19
POPC:POPS (5:1)/K ⁺	CHARMM36 ^{5,17}	0.45	110:22	4926	40	298	200	150	20
POPC:POPS (5:1)/K ⁺	CHARMM36 ^{5,17}	0.89	110:22	4946	79	298	200	150	21
POPC:POPS (5:1)/Na ⁺	CHARMM36 ^{5,17}	0	110:22	4620	0	298	500	100	22
POPC:POPS (5:1)/Na ⁺	CHARMM36 ^{5,17}	0.44	110:22	4965	39	298	200	150	23
POPC:POPS (5:1)/Na ⁺	CHARMM36 ^{5,17}	0.89	110:22	4932	79	298	200	150	24
POPC:POPS (5:1)/K ⁺	MacRog ²⁵	0	120:24	5760	0	298	400	250	26
POPC:POPS (5:1)/K ⁺	MacRog ²⁵	0.50	120:24	5760	52	298	300	200	27
POPC:POPS (5:1)/K ⁺	MacRog ²⁵	1.00	120:24	5760	104	298	300	200	27
POPC:POPS (5:1)/K ⁺	MacRog ²⁵	2.00	120:24	5760	208	298	300	200	27
POPC:POPS (5:1)/K ⁺	MacRog ²⁵	3.00	120:24	5760	311	298	300	200	27
POPC:POPS (5:1)/K ⁺	Lipid14/17 ^{28,29}	0	120:24	5760	0	298	500	200	30
POPC:POPS (5:1)/K ⁺	Lipid14/17 ^{28,29}	0.50	120:24	5760	54	298	300	200	31
POPC:POPS (5:1)/K ⁺	Lipid14/17 ^{28,29}	1.00	120:24	5760	104	298	300	200	31
POPC:POPS (5:1)/K ⁺	Lipid14/17 ^{28,29}	2.00	120:24	5760	208	298	300	200	31
POPC:POPS (5:1)/K ⁺	Lipid14/17 ^{28,29}	3.00	120:24	5760	311	298	300	200	31
POPC:POPS (5:1)/K ⁺	Lipid14/17 ^{28,29}	4.00	120:24	5760	415	298	300	200	31
POPC:POPS (5:1)/Na ⁺	Lipid14/17 ^{28,29}	0	120:24	5760	0	298	500	200	32
POPC:POPS (5:1)/Na ⁺	Lipid14/17 ^{28,29}	0.50	120:24	5760	54	298	300	200	33
POPC:POPS (5:1)/Na ⁺	Lipid14/17 ^{28,29}	1.00	120:24	5760	104	298	300	200	33
POPC:POPS (5:1)/Na ⁺	Lipid14/17 ^{28,29}	2.00	120:24	5760	208	298	300	200	33
POPC:POPS (5:1)/Na ⁺	Lipid14/17 ^{28,29}	3.00	120:24	5760	311	298	300	200	33
POPC:POPS (5:1)/Na ⁺	Lipid14/17 ^{28,29}	4.00	120:24	5760	415	298	300	200	33
POPC:POPS (4:1)/Na ⁺	Berger ^{34,35}	0	102:26	4290	0	310	120	80	36
POPC:POPS (4:1)/Na ⁺	Berger ^{34,35}	1.03	102:26	4290	80	310	200	50	37

^aExcess Na⁺ or K⁺ concentration

^bNumber of lipid molecules

^cNumber of water molecules

^dNumber of additional cations

^eSimulation temperature

^fTotal simulation time

^gTime used for analysis

^hReference for simulation files

POPC:POPS (5:1) mixtures with additional calcium using the NBfix2 parameters. POPC:POPS (5:1) mixtures containing a total of 300 (250:50) lipids, neutralizing sodium ions, and 0.14 M or 0.94 M CaCl_2 were prepared using the CHARMM-GUI in August 2019.^{3,4} The ion parameters generated by the CHARMM-GUI at the time are labeled here as NBfix2.³⁹ Systems were simulated using Gromacs 2018.6⁸ and the CHARMM36 force field with simulation parameters given by the CHARMM-GUI at 320 K.

S1.2 CHARMM36-UA

DOPS and POPS bilayers. Starting structures were taken from those generated for the CHARMM36 simulations (see section S1.1), with any extraneous hydrogen atoms removed in the lipid tails. Force field parameters for DOPS and POPS were constructed through a combination of the published CHARMM36 PS⁵ and CHARMM36-UA PC parameters.⁴⁰ All other simulation parameters and conditions were identical to those described for the CHARMM36 all-atom DOPS and POPS simulations.

S1.3 MacRog

POPC bilayers. The POPC bilayer consisting of a total of 128 lipids was constructed from a single lipid structure taken from Ref. 41. The bilayer was hydrated by a total of 5120 water molecules, corresponding to 40 water molecules per lipid. The MacRog lipid parameters,⁴² obtained from Ref. 41, were used, along with the TIP3P water model.⁴³ The simulation parameters were identical to those used for POPC:POPS (5:1) mixtures with the MacRog force field, see further below in this section. The simulation was run for 200 ns using Gromacs 2016.3,⁸ out of which the last 150 ns were used for analysis. The simulation data and related files are available from Ref. 44.

POPS bilayers with Na^+ counterions. Force field parameters for POPS simulations with the MacRog OPLS-AA force field^{25,42,45} were constructed manually using the PS parameters

provided in ref. 45 as a guide. The original parameters were not used due to an incorrect arrangement of the *sn*-1 and *sn*-2 tails (i.e. the lipid was OPPS and not POPS). The corrected parameters are available from Ref. 46. The starting structure was the same as that used in the CHARMM36 POPS simulations (with Na^+ ions), and was converted into the correct format using a script to adjust the atom order. Water was treated using the TIP3P model.⁴³ Simulation parameters were chosen to closely mimic those used in the original force field publications:^{25,42,45} van der Waals interactions were truncated at 1.0 nm with a dispersion correction applied to the energy and pressure; long-range Coulombic interactions were treated with PME beyond a system-optimized cut-off. All other simulation settings were identical to those described above in section S1.1 for the CHARMM36 DOPS and POPS simulations, including the use of the Verlet cut-off scheme,⁴⁷ except that here LINCS was used to constrain all bonds. Simulations with the group cut-off scheme gave slightly lower area per molecule ($\sim 50 \text{ \AA}^2$) than the simulations with the Verlet cut-off ($\sim 52 \text{ \AA}^2$).

POPS bilayers with K^+ counterions. The membrane with sodium counterions was further simulated after replacing Na^+ counterions by K^+ ones, which were described by the Åqvist parameters.⁴⁸ Other topologies were unchanged. Simulation parameters were the same as used for the POPC:POPS (5:1) mixtures with the MacRog force field, see further below in this section. The simulation was run for 200 ns, out of which the last 150 ns was used in the analysis.

POPC:POPS (5:1) mixtures with additional potassium ions. Bilayers containing a total of 120 POPC and 24 POPS molecules distributed evenly among the two leaflets were set up using CHARMM-GUI.^{3,4} The bilayers were solvated by 5760 water molecules, corresponding to 40 water molecules for lipid. Additionally, 24 potassium ions were added to neutralize the charge of the POPS head groups. These bilayers were simulated using Gromacs 2016.3⁸ in the presence of counterions only, as well as together with different concentrations of CaCl_2 or KCl . For the former, concentrations of 100 mM, 300 mM, 1 M, and 3 M were considered, which corresponded to the amounts of 10/20, 31/62, 104/208, and 311/622 of $\text{Ca}^{2+}/\text{Cl}^-$ ions.

For membranes with KCl, concentrations of 500 mM, 1 M, 2 M, and 3 M of were considered, corresponding to 52, 104, 208, and 311 pairs of K^+ and Cl^- ions.

The lipids were described using the MacRog model.^{25,42,45} The POPC topologies were obtained from Ref. 41, whereas the POPS topology was adapted from the OPPS topology in Ref. 45 by reversing the order of the acyl chains. The initial structures from CHARMM-GUI were used, because they had the naturally occurring L stereoisomer in the POPS head group, instead of the the D stereoisomer present in Ref. 45. The TIP3P model⁴³ was used for water, and the Åqvist parameters,⁴⁸ standard for the OPLS force field, were employed for the ions.

Simulation parameters were taken from Ref. 45. Periodic boundary conditions were employed in all dimensions. The neighbor list was updated every step. The Lennard-Jones interactions were cut off at 1 nm, whereas the smooth particle mesh Ewald algorithm¹⁵ was used for long-range electrostatics. Dispersion correction⁴⁹ was applied to both energy and pressure. Temperature was kept at 298 K using the Nosé–Hoover thermostat.^{11,12} The lipids and the solvent were coupled separately, and a time constant of 0.4 ps was employed. Pressure was maintained semi-isotropically at 1 bar using the Parrinello–Rahman barostat with a time constant of 1 ps.¹³ All non-water bonds were constrained with the LINCS algorithm,^{9,10} whereas the bonds in water molecules were constrained using SETTLE.⁵⁰ The integration time step was set to 2 fs, and the simulations were performed either for 400 ns (only counterions), 300 ns (systems with KCl), or 600 ns (systems with CaCl_2). The last 250, 200, or 300 ns of the simulations were included in the analysis, respectively.

S1.4 Lipid17

DOPS and POPS bilayers. The structures of the bilayers with 128 DOPS or 128 POPS lipids were obtained from CHARMM-GUI.^{3,4} Bilayers were solvated with 4480 water molecules, resulting in 31.1 waters per lipid. For each system, 128 Na^+ ions were added to neutralize the system. In all simulations, TIP3P⁵¹ was used as the solvent. The SETTLE⁵⁰ algorithm was employed to constrain the bonds in TIP3P water molecules. Simulations were run using

the Amber18 simulation package,⁵² and lipid parameters were obtained from the Amber Lipid17 force field.²⁹ For the ions, one set of simulations were run with the Joung–Cheatham ion parameters⁵³ and another set of simulations with the ff99SB (Åqvist)⁴⁸ ion parameters. The data in Table 1 and Refs. 54–57 contain the number of molecules in simulations, related simulation files, and trajectories.

Each bilayer structure was first minimized for 2500 steps using the steepest descent algorithm and then an additional 2500 steps with the conjugate gradient algorithm while restraining the solvent and ions with a force constant 500 kcal mol⁻¹ Å⁻². An additional minimization step was used with the same parameters after removing the constraints on the solvent and ion molecules. During the minimization procedure, non-periodic boundary conditions were applied, no pressure scaling was used and none of the bonds were restrained. A three-step heating procedure was applied: In the first heating step, at constant volume without periodic boundary conditions, the system temperature was increased from 0.0 K to 100.0 K using Langevin thermostat with 5.0 ps⁻¹ collision frequency, while restraining the lipid positions with harmonic springs of force constant 20.0 kcal mol⁻¹ Å⁻¹. In the second heating step, at constant volume, the system temperature was increased from 100.0 K to 200.0 K using Langevin thermostat with 5.0 ps⁻¹ collision frequency within 10 000 steps, while restraining the lipid positions with harmonic springs of force constant 10.0 kcal mol⁻¹ Å⁻¹. In the third heating step, the system temperature was increased from 200.0 K to 303.0 K within 10 000 steps using Langevin thermostat with 5.0 ps⁻¹ collision frequency, while restraining the lipid positions with harmonic springs of force constant 10.0 kcal mol⁻¹ Å⁻¹ at 1 bar constant pressure using Berendsen barostat with 3.0 ps relaxation time. From the second heating step onward, periodic boundary conditions in all dimensions were applied. Semi-isotropic pressure coupling along *xy*-plane was employed, and surface tension was set to 0.0 dyn explicitly. After the third heating step, each structure was equilibrated for 100 ns at 1 bar and 303 K using Berendsen barostat and Langevin thermostat. For the equilibration step, semi-isotropic pressure coupling along *xy*-plane was employed, and the surface tension was

set to 0.0 dyn explicitly. For all heating and equilibration steps, the lengths of the hydrogen containing-bonds were restrained using the SHAKE algorithm; time step of 2 fs was used. In all steps with periodic boundary conditions, the non-bonded interactions were calculated with particle mesh Ewald¹⁵ using 1.0 nm cutoff.

For the production runs, temperature and pressure were set to 303 K and 1 bar, using Langevin thermostat with 1.0 ps⁻¹ collision frequency and Berendsen barostat with 1.0 ps relaxation time. Periodic boundary conditions were applied in all dimensions, and the non-bonded interactions calculated with particle mesh Ewald¹⁵ using 1.0 nm cutoff. The lengths of the hydrogen-containing bonds were constrained using the SHAKE algorithm. Time step of 2 fs was used. Trajectories were saved at 10 ps intervals. Two independent 500 ns long trajectories were generated, of which the last 200 ns was used for the analysis.

POPC:POPS (5:1) mixtures with additional potassium and sodium ions. The initial structures of the bilayers with 120 POPC and 24 POPS lipids were obtained from CHARMM-GUI.^{3,4} Bilayers were solvated with 5760 TIP3P water molecules.⁵¹ For the simulations of the lipids and ions, the Amber Lipid17²⁹ and ff99SB⁴⁸ force fields were used, respectively. Simulations were run using the Amber18 simulation package.⁵² The simulation steps were the same as for the simulations of the DOPS and POPS bilayers described above in this section, with the only difference that the total simulation time was 300 ns, of which the last 200 ns was used for the analysis. The number of ions in each specific system is given in Table S1. The trajectory files can be found in Refs. 30–33.

POPC:POPS (5:1) mixtures with additional CaCl₂ using default Amber parameters. Simulations were performed using the Amber18 simulation package⁵² with the ff99SB⁴⁸ ion parameters and the Amber Lipid17²⁹ force field. Number of ions and water molecules for this set of simulations are shown in Table 2. The simulation details, minimization, heating, and equilibration runs were the same as described above in this section for the other POPC:POPS (5:1) simulations with the Amber Lipid17 forcefield. For each ion concentration, 100 ns equilibration runs were followed by 300 ns production runs with two independent trajectories,

of which last 200 ns were used for the analysis. The trajectory files can be found in Ref. 58.

POPC:POPS (5:1) mixtures with additional CaCl₂ using Dang ion parameters. The Lipid17 parameters for POPS were obtained from AmberTools18⁵² and converted to Gromacs format using acpype.⁵⁹ The previously generated¹ Lipid14 parameters for POPC in Gromacs format were downloaded from Ref. 60. Dang parameters for ions^{61,62} were used. Initial structures were generated using CHARMM-GUI,^{3,4} and simulations were performed using the Gromacs 2018 simulation package⁸ with time step of 2 fs. The non-bonded interactions were calculated directly within 1.0 nm cutoff; the Verlet scheme was used;⁴⁷ and the long-range electrostatic forces were calculated using particle mesh Ewald.¹⁵ The bond lengths of hydrogen atoms were constrained using LINCS.⁹ Temperature was coupled to the velocity rescaling thermostat⁶³ at 298 K with a coupling constant of 1 ps. Pressure was coupled to the Parrinello–Rahman barostat¹³ at 1 bar with a coupling constant of 10 ps. The compositions of individual simulations are shown in Table 2. The systems were equilibrated 50 ns prior to production simulations, which are available in Ref. 64 together with the simulation settings. Topologies in Gromacs format are available in the repository of Ref. 65.

S1.5 Slipids

POPS and DOPS with 128 lipids. Starting structures were the same as for the CHARMM36 simulations, see section S1.1. Force field parameters were taken from the published Slipids PS model,⁶⁶ however simulation cut-offs used herein were different to these previously published simulations.⁶⁷ This was due to the use of the older GROMACS group-based cut-off scheme in those previous simulations. In the simulations reported in this work, the Verlet cut-off scheme was used. Van der Waals interactions were truncated at 1.0 nm with LJ-PME⁶⁸ applied to account for the long-range interactions. Coulombic interactions were truncated at 1.0 nm with PME used for the long-range interactions. Full testing and validation of these settings with the Slipids PS force field will be provided in an additional forthcoming work. All other simulation settings were identical to those described above (section S1.1) for the

CHARMM36 DOPS and POPS simulations.

DOPS with 288 lipids. The starting structure with 288 DOPS lipids, 11232 water molecules and 288 Na⁺ ions was constructed with the MEMBRANE BUILDER website.⁶⁹ The Slipids⁶⁶ forcefield was used for DOPS, the TIP3P⁴³ water model was used to solvate the system, and ions were described by the parameters derived by Åqvist.⁴⁸ The system was simulated in NPT ensemble for 200 ns using the GROMACS 5.0.4 package,⁸ and the last 100 ns was used for the analysis. Timestep of 2 fs was used with the leapfrog integrator. The Nosé–Hoover thermostat^{11,12} was used with reference temperature of 303 K and a relaxation time constant of 0.5 ps; lipids and water plus ions were coupled separately to the heat bath. Pressure was controlled at 1.013 bar using a semi-isotropic Parrinello–Rahman barostat¹³ with a time constant of 10.0 ps. Long-range electrostatic interactions were calculated using the PME method.^{14,15} A real space cut-off of 1.0 nm was employed with grid spacing of 0.12 nm in the reciprocal space. Lennard-Jones potentials were cut off at 1.4 nm, with a dispersion correction applied to both energy and pressure. All covalent bonds in lipids were constrained using the LINCS algorithm,⁹ whereas water molecules were constrained using SETTLE.⁵⁰ Twin-range cutoffs, 1.0 nm and 1.6 nm, were used for the neighbor lists with the long-range neighbor list updated every 10 steps.

S1.6 Berger

POPC bilayer. Previously published simulation⁷⁰ from Ref. 71 was used for POPC at 310 K.

DOPS and POPS bilayers. Starting structures for simulations performed with a Berger-based PS force field were taken from those produced for the CHARMM36 simulations, see section S1.1 above. A script was used to re-order the atoms and to remove any extraneous hydrogen atoms. Force field parameters were taken from those published by Mukhopadhyay et al.,³⁵ and the SPC water model was used.⁷² The simulation cut-offs closely matched those of Mukhopadhyay et al.: van der Waals interactions were truncated at 1.0 nm; Coulombic interactions were truncated at 1.0 nm, with PME to account for the interactions beyond the

cut-off. All other simulation settings were identical to those described above (section S1.1) for the CHARMM36 DOPS and POPS simulations, including the use of the Verlet cut-off scheme, except that here LINCS was used to constrain all bonds.

POPC:POPS (4:1) mixtures with additional sodium and calcium ions. Previously published simulations with additional amount of sodium,⁷³ available from Ref. 37, and with additional amounts of calcium,⁷⁴ available from Refs. 75,76, were used. To generate the reference system with sodium counterions only, the additional ions were removed from the structure file in Ref. 37. This system was simulated 120 ns using Gromacs 5⁸ with parameter (mdp) and force field (top and itp) files available from Ref. 36. The last 80 ns of the trajectory was used for the analysis.

S1.7 GROMOS-CKP and GROMOS-CKPM

The GROMOS-CKP force field (CKP stands for Chandrasekhar–Kukol–Piggot) contains a set of GROMOS-compatible lipid parameters. Parameters have been developed and validated for PC,^{77–79} PE, PG, cardiolipin⁸⁰ and PI⁸¹ lipids, amongst others. Within this work we provide an initial validation for simulating PS lipids with two variants of this force field (termed GROMOS-CKP and GROMOS-CKPM). Additional forthcoming work will provide additional validation and testing of these PS parameters. The two variants of the force field only differ in terms of the charges in the head group. The GROMOS-CKPM (M stands for Mukhopadhyay after the first Berger-based PS simulations published) lipid uses Berger/Chiu-based charges for the NH₃ part of the PS head group (i.e., has the same charges as used in the choline part of the Berger PC lipids). The GROMOS-CKP parameters use charges compatible with the rest of the GROMOS force fields; the charges of the NH₃ part of the PS head group were taken from a lysine side-chain of the GROMOS 54A7 protein force field.⁸² The remainder of the parameters were assigned by analogy from either the other GROMOS-CKP lipids or the GROMOS 54A7 force field.

DOPS and POPS bilayers. Starting structures were taken from those produced for the

CHARMM36 simulations, see section S1.1 above. A script was used to re-order the atoms and to remove any extraneous hydrogen atoms. The force field parameters for DOPS and POPS were as discussed in the beginning of the present section. The SPC water model was used in these simulations.⁷² Simulation cut-offs were chosen to closely match those used in the original GROMOS-CKP force field validation: van der Waals interactions were truncated at 1.4 nm with dispersion corrections applied to energy and pressure; Coulombic interactions were also truncated at 1.4 nm, with PME used to treat the long-range interactions. All other simulation settings were identical to those described above (section S1.1) for the CHARMM36 DOPS and POPS simulations, including the use of the Verlet cut-off scheme, except that here LINCS was used to constrain all bonds.

POPC:POPS (5:1) mixtures without additional ions. Starting structures for GROMOS-CKP and GROMOS-CKPM simulations were taken from those produced for the equivalent CHARMM36 simulations (see section S1.1 above). A script was used to re-order the atoms and to remove any extraneous hydrogen atoms. Simulation settings were identical to those described previously in the present section for the GROMOS-CKP(M) POPS bilayers.

S2 Molecular electrometer in PC lipid bilayers mixed with negatively charged lipids

The molecular electrometer concept is based on the empirical observations that the C–H bond order parameters of α and β carbons in PC lipid headgroup decrease (increase) proportionally to the bound positive (negative) charge^{83–86} (Fig. S1). Therefore, the headgroup order parameters can be used to measure the ion binding affinity to lipid bilayers containing PC lipids.^{16,83–85,87,88} Changes of the headgroup order parameters of negatively charged PS and PG lipids are also systematic, but not as well characterized^{16,87–89} than for PC, and the ion binding affinity to negatively charged bilayers can be better quantified by measuring the PC headgroup order parameters from mixed bilayers.^{16,87–90}

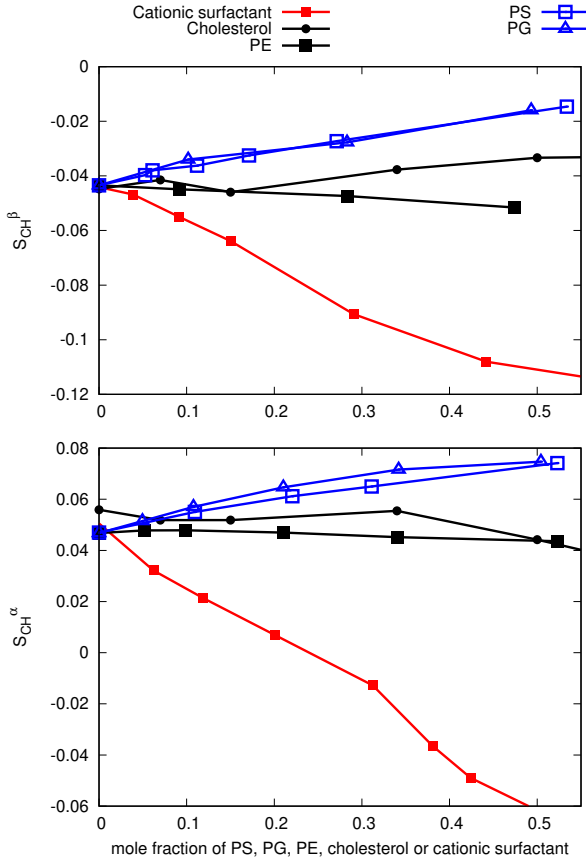


Figure S1: Headgroup order parameters S_{CH}^β and S_{CH}^α of POPC measured from mixtures with PS (bovine brain), POPG, POPE, cholesterol, and cationic dihexadecyldimethylammonium bromide (DHAB) surfactant.^{86,91,92} Signs are taken from separate experiments.^{93,94}

When using the PC headgroup S_{CH} to evaluate the ion binding affinity to a bilayer containing anionic lipids, it is important to note that these S_{CH} increase due to the addition of negative charged lipids according to the molecular electrometer^{85,91} (Fig. S1). Therefore, the PC headgroup order parameters are larger in mixtures with anionic lipids than in pure PC lipid bilayers, as seen from Fig. S2 by comparing the measurements without added salt. Upon addition of CaCl_2 , the S_{CH} decrease and reach the values of pure PC bilayers around CaCl_2 concentrations of $\sim 50\text{--}300$ mM, depending on the amount of negatively charged lipids in the mixture (Fig. S2). Around these concentrations the positive charge of the bound Ca^{2+} cancels the negative charge of the lipids, resulting in a neutral membrane. Above these concentrations, the specific binding of calcium leads to overcharging of the membrane.

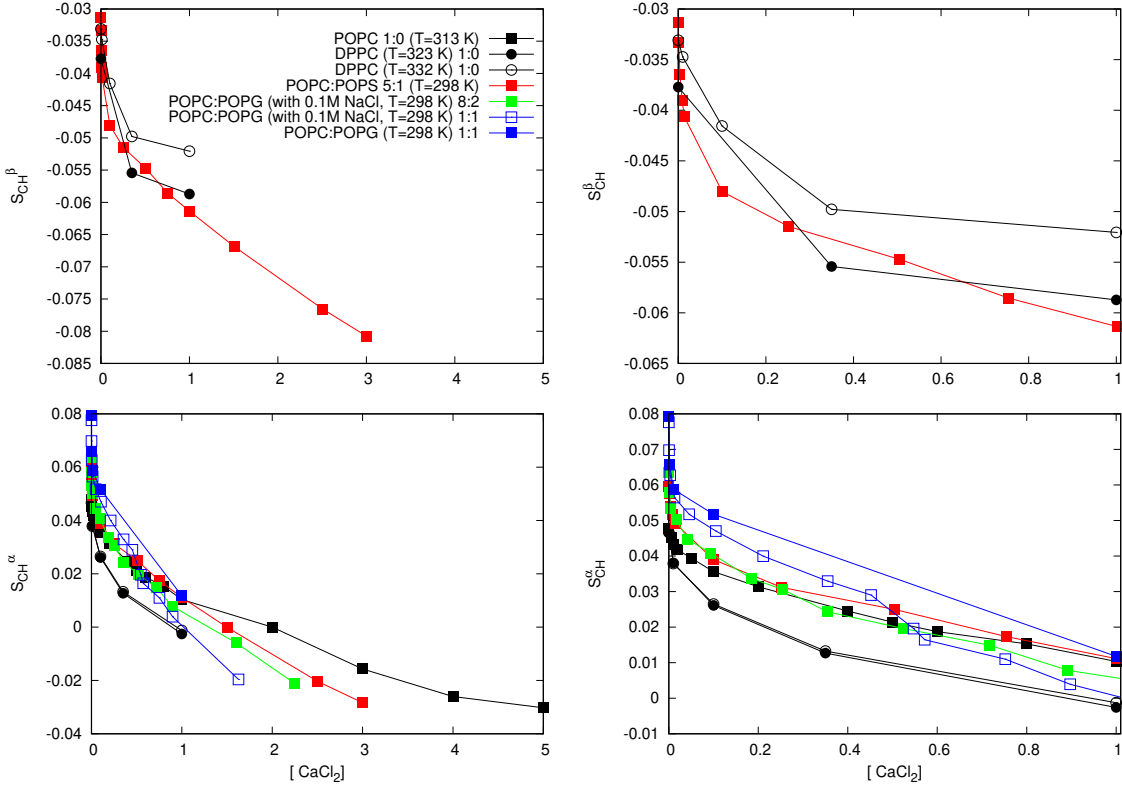


Figure S2: Headgroup order parameters of POPC as a function of CaCl_2 concentration from experiments with different mole fractions of negatively charged lipids (left column). Right column shows the same data zoomed to the concentrations below 1 M. Data for pure DPPC from Ref. 83, for pure POPC from Ref. 84, for POPC:POPS (5:1) mixture from Ref. 16, for POPC:POPG (8:2:1:1) mixtures with 0.1 M NaCl from Ref. 88, and for POPC:POPG (1:1) mixture without NaCl from Ref. 87.

Because the POPC headgroup S_{CH} in mixtures with different amounts of anionic lipids but without additional salt are not equal, the binding affinity of calcium can be better compared by plotting the changes of order parameters, ΔS_{CH} , as a function of added calcium. As expected, such a plot reveals more pronounced order parameter decrease in systems with larger fractions of negatively charged lipids (Fig. S3), indicating an increase in the calcium binding affinity with the increasing amount of negatively charged lipids in membranes. In conclusion, the presented empirical comparison of headgroup order parameter changes from various mixtures of POPC and anionic lipids with added calcium gives physically consistent results, suggesting that the molecular electrometer can be used to determine the cation binding affinity also to lipid bilayers containing mixtures of PC and anionic lipids.

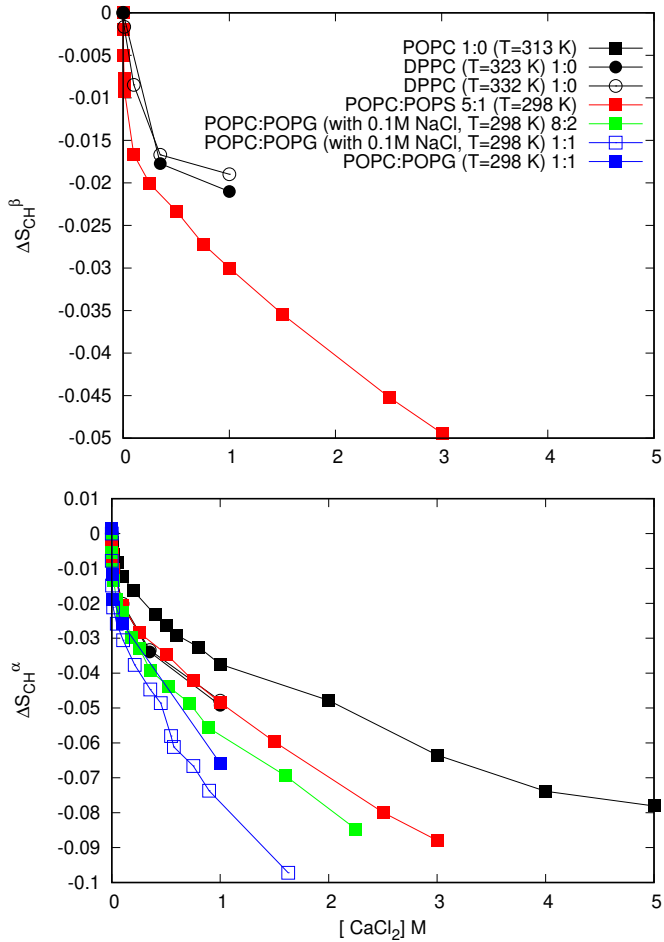


Figure S3: Changes of POPC headgroup order parameters, $\Delta S_{\text{CH}}^\beta$ and $\Delta S_{\text{CH}}^\alpha$, as a function of CaCl_2 measured from mixed bilayers containing different amounts of anionic lipids. The original data are the same as in Fig. S2.

S3 Calibration of PC headgroup order parameter response to bound cations

When using the molecular electrometer to compare ion binding affinity between simulations and experiments, one needs to keep in mind that two things affect how much a given S_{CH} changes when the charge content of a solution is varied: 1) the change in the amount of bound charge, and 2) the sensitivity of the S_{CH} to bound charge. Therefore, the response of the order parameters to bound charge in simulations needs to be first calibrated against experiments.^{95,96}

In our previous work,⁹⁵ we investigated the change in order parameters under varying concentrations of monovalent and divalent salts and concluded that the experimental $\Delta S_{\text{CH}}^{\beta}/\Delta S_{\text{CH}}^{\alpha}$ ratio⁸³ was well reproduced by Lipid14, but underestimated by other force fields. In a more recent study,⁹⁶ the headgroup order parameter responses were compared more carefully against experiments of cationic dihexadecyldimethylammonium bromide (DHAB) surfactants in POPC bilayer.⁸⁶ The advantage of this approach is that the amount of DHAB in the bilayer is exactly known in experiments, which can be exploited to extract the sensitivity of the order parameters. This revealed that both S_{CH}^{β} and S_{CH}^{α} in Lipid14 are equally oversensitive (thus giving the correct $\Delta S_{\text{CH}}^{\beta}/\Delta S_{\text{CH}}^{\alpha}$) to the bound charge, whereas CHARMM36 gives better agreement for the α carbon (Fig. S4), indicating that the headgroup order parameter response to bound charge is actually more realistic in CHARMM36 than in Lipid14. The ratio was overestimated for CHARMM36, because the β -carbon order parameter is relatively more sensitive than the α -carbon order parameter.

That being said, in the force fields investigated so far, the discrepancies arising from the sensitivity of lipid headgroup to bound charge are typically smaller than the discrepancies arising from ion binding affinity.

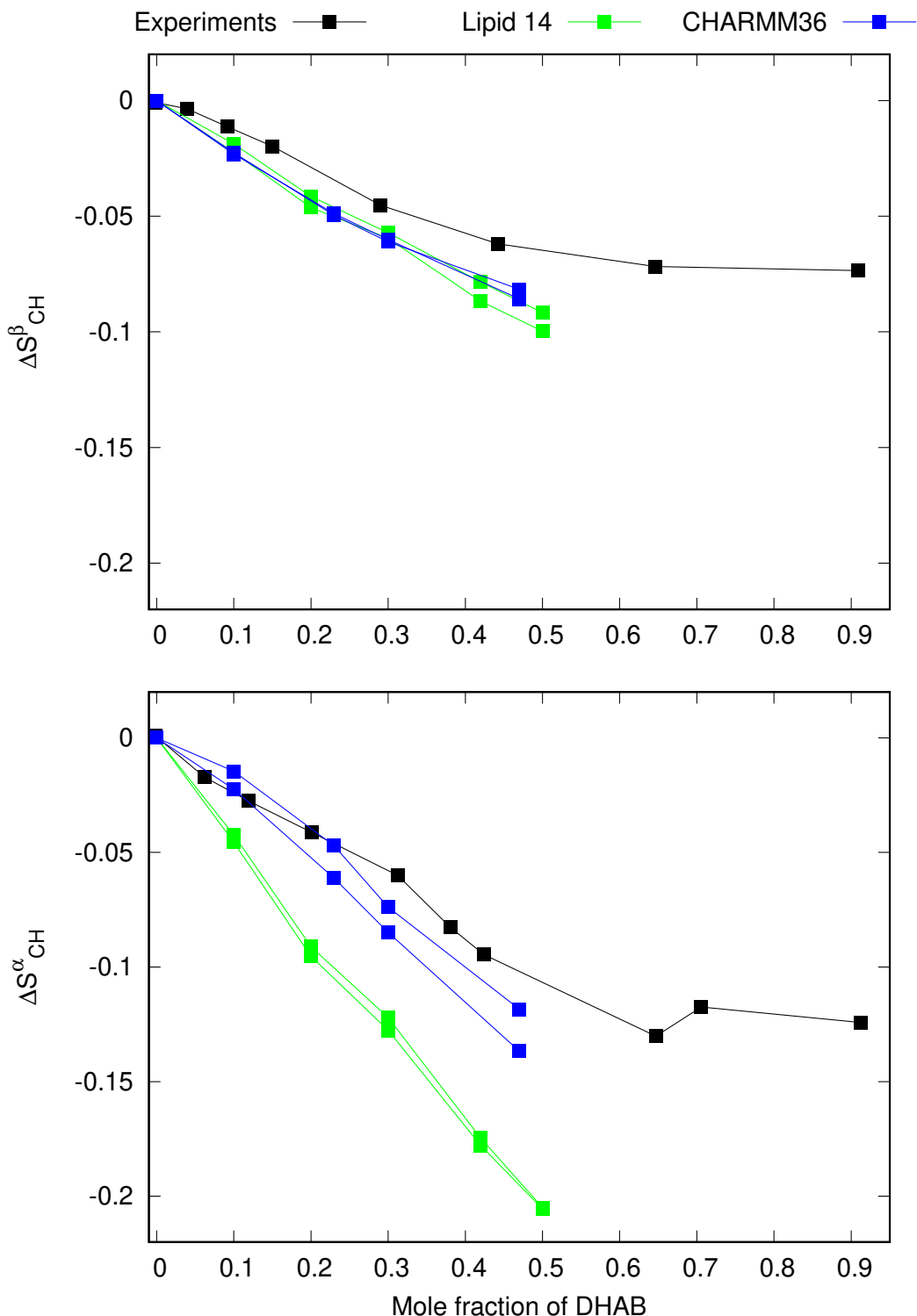


Figure S4: Responses of headgroup order parameters to cationic surfactant in POPC bilayer from simulations and experiments.⁸⁶ The simulation results for Lipid14 are from Ref. 96. The CHARMM36 simulation data and details are available from Ref. 97.

S4 Sensitivity of molecular electrometer on the definition of ion concentration

Previous studies using the molecular electrometer to assess ion binding affinity to lipid bilayers report ion concentrations either 1) in water before solvating the lipids (buffer concentration),^{16,83,95} or 2) in bulk water after solvating the lipids (bulk concentration).^{84,96} In this work, we use the definition 1) to be consistent with the experimental reference data.¹⁶ The difference between these two definitions increases with increasing ion binding affinity. However, Fig. S5 demonstrates that in a force field with a realistic ion binding affinity⁹⁶ the deviation between the two definitions is negligible.

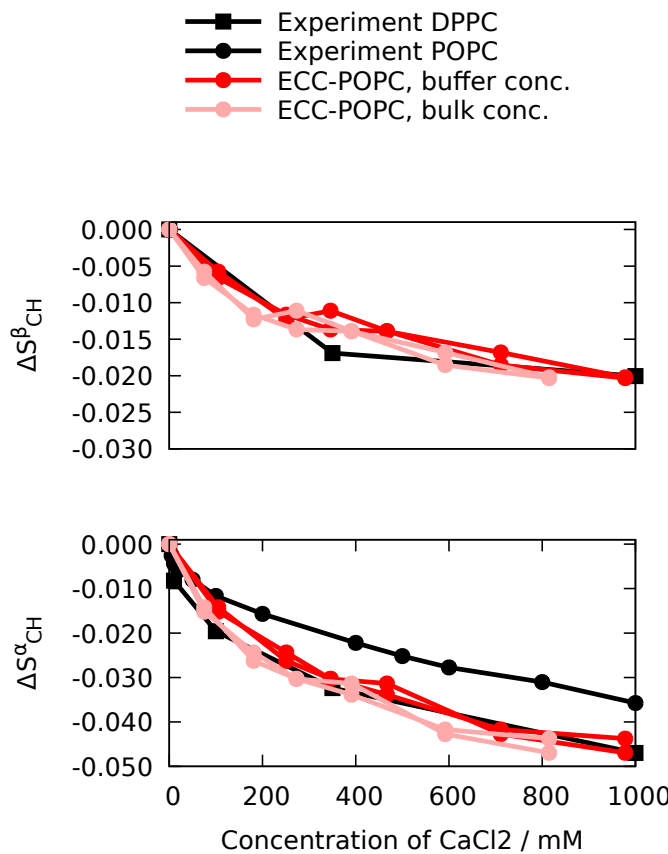


Figure S5: Changes of the headgroup order parameters as a function of CaCl_2 concentration using two possible definitions of ion concentration. Data from a recent force field with realistic calcium binding affinity to a POPC bilayer⁹⁶ shown together with the experimental data.^{83,84}

S5 Spectral slices in indirect dimension from R-PDLF and S-DROSS experiments

The C–H bond order parameters of the headgroup and glycerol backbone carbons were determined as $S_{\text{CH}} = \Delta\nu / (0.315 \times 21.5\text{kHz})$, where $\Delta\nu$ is the dipolar splitting given by the largest peak widths observed in the second dimension of the R-PDLF spectra (blue lines in Fig. S6), 0.315 is the scaling factor of the R18 recoupling sequence and 21.5 kHz is the maximum ^1H – ^{13}C dipolar coupling for a C–H bond.⁹⁸ The resulting order parameters were in good agreement with the previously reported values from ^2H NMR experiments⁹⁹ (Fig. 2 in the main text). However, the resolution in our ^{13}C NMR experiment was not sufficient to detect the splitting related to the smaller order parameter of the C–H bond in the α -carbon that has been observed in ^2H NMR experiments.⁹⁹ Therefore, the value of 0 ± 0.02 from our ^{13}C NMR experiments is shown in Fig. 2 in the main text, and the magnitude of 0.02 from literature is used in the SIMPSON calculations in the main text.

Interpretation of the α -carbon order parameter signs of from the S-DROSS experiment is complicated by the presence of distinct order parameters for the two attached hydrogens. As discussed in the main text, interpretation of the S-DROSS curve with the help of SIMPSON simulations gave values +0.09 and –0.02 for the α -carbon order parameters. To corroborate our interpretation, we measured the S-DROSS curve also using the higher 8 kHz MAS frequency (Fig. S6 bottom), which makes the experiment more sensitive to larger order parameter values. Also this experiment indicated a positive value for the larger α -carbon order parameter.

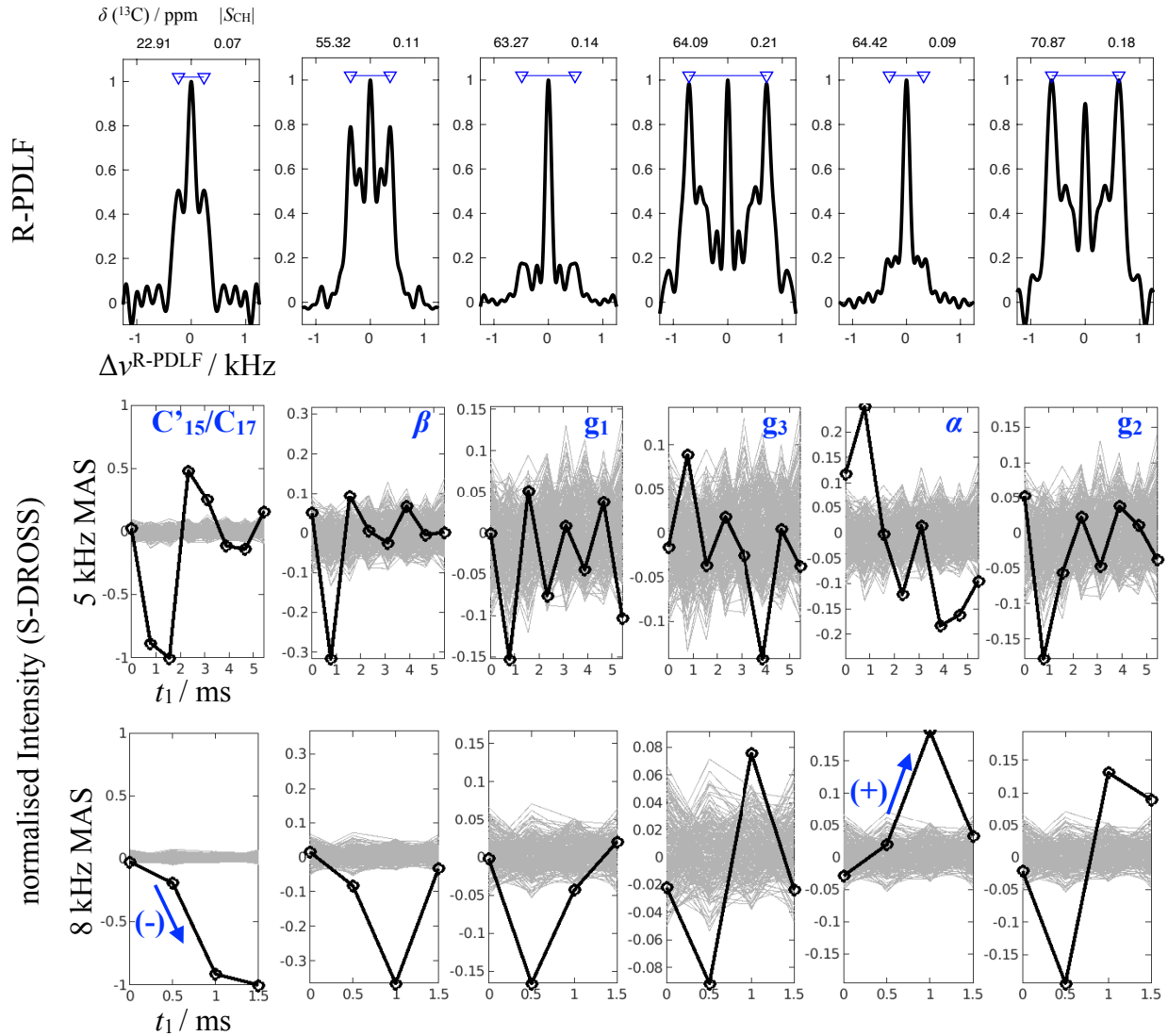


Figure S6: Spectral slices in indirect dimension from the R-PDLF (top row) and S-DROSS (middle and bottom rows) experiments at distinct chemical shifts. The chemical shifts and order parameters (calculated from the dipolar splittings indicated with blue lines in the R-PDLF slices) are written on top of each column (chemical shift left, order parameter right). The assignment of columns is given with blue text in the middle row panels. The S-DROSS slices were measured using both the 5 kHz (middle row) and 8 kHz (bottom row) MAS frequencies to enable higher sensitivity to the order parameters with lower and higher magnitudes, respectively. The background noise taken from chemical shift slices without carbon peaks (grey lines in S-DROSS figures) were used to determine the error bars for the α and β carbons in Fig. 1 in the main text. The S-DROSS profile of the acyl chain methyl carbons (leftmost column) was used as reference assuming that these carbons have negative order parameters.

S6 Dihedral angle distributions in headgroup and glycerol backbone regions of PS lipids from different simulation models

The dihedral angle distributions (Figs. S7 and S8) and structures (Fig. S9) of the glycerol backbone and headgroup regions of POPS lipids showed a wide variety between different MD force fields. Detailed discussion on the relevance of the observed structural differences is limited by the lack of a realistic force field (that would correctly reproduce the headgroup and glycerol backbone C–H bond order parameters, S_{CH}). However, some structural characteristics of the PS headgroup can be suggested based on the best available models for it (Figs. S10, S11 and S12), as discussed in the main text. The glycerol backbone structures are not discussed in this work, because our focus is on the PS headgroup. However, the data presented here can be useful for future investigations.

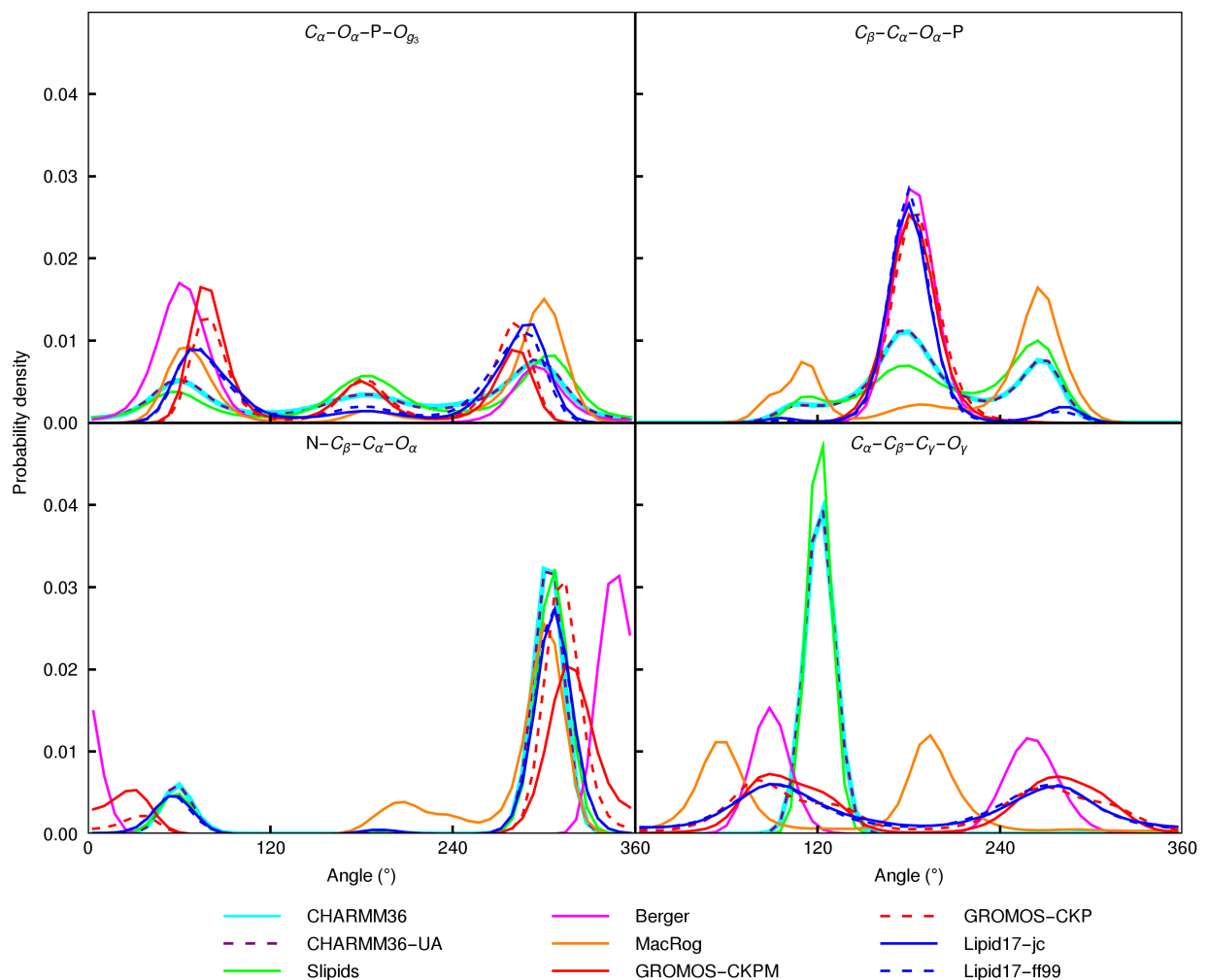
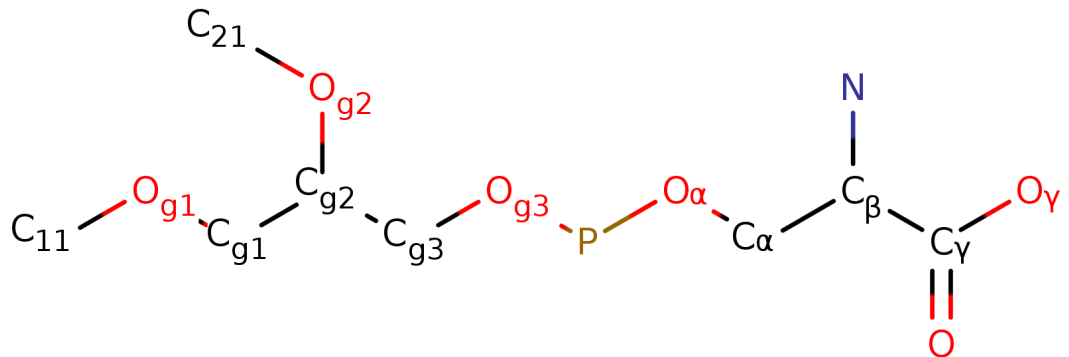


Figure S7: Dihedral angle distributions in the headgroup region of POPS from different simulation models.

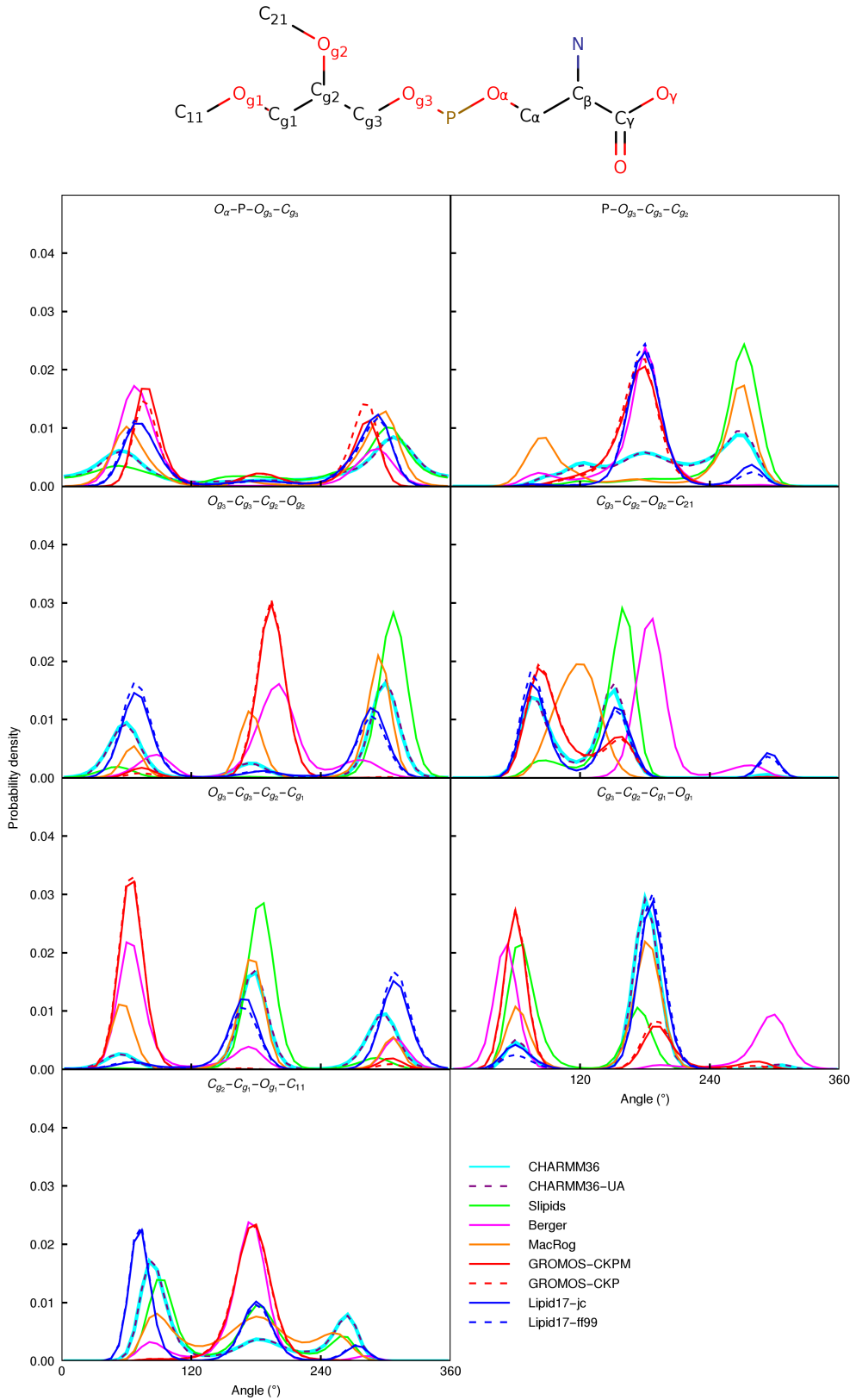


Figure S8: Dihedral angle distributions in the glycerol backbone region of POPS from different simulation models.

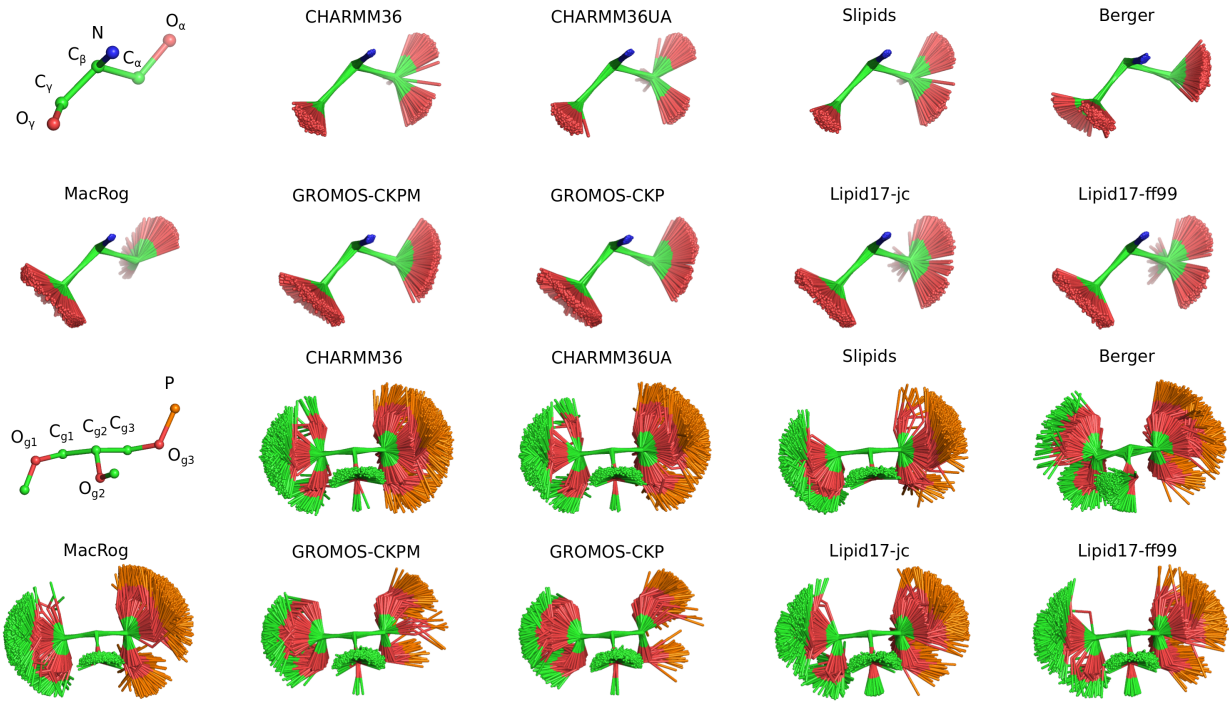


Figure S9: Overlayed snapshots of the headgroup (C_{γ} - C_{β} - C_{α} carbons overlayed) and glycerol backbone (C_{g_1} - C_{g_2} - C_{g_3} carbons overlayed) regions from POPS simulations with different force fields. Note that only one of the two O_{γ} atoms in the carboxylate group of PS lipids is shown.

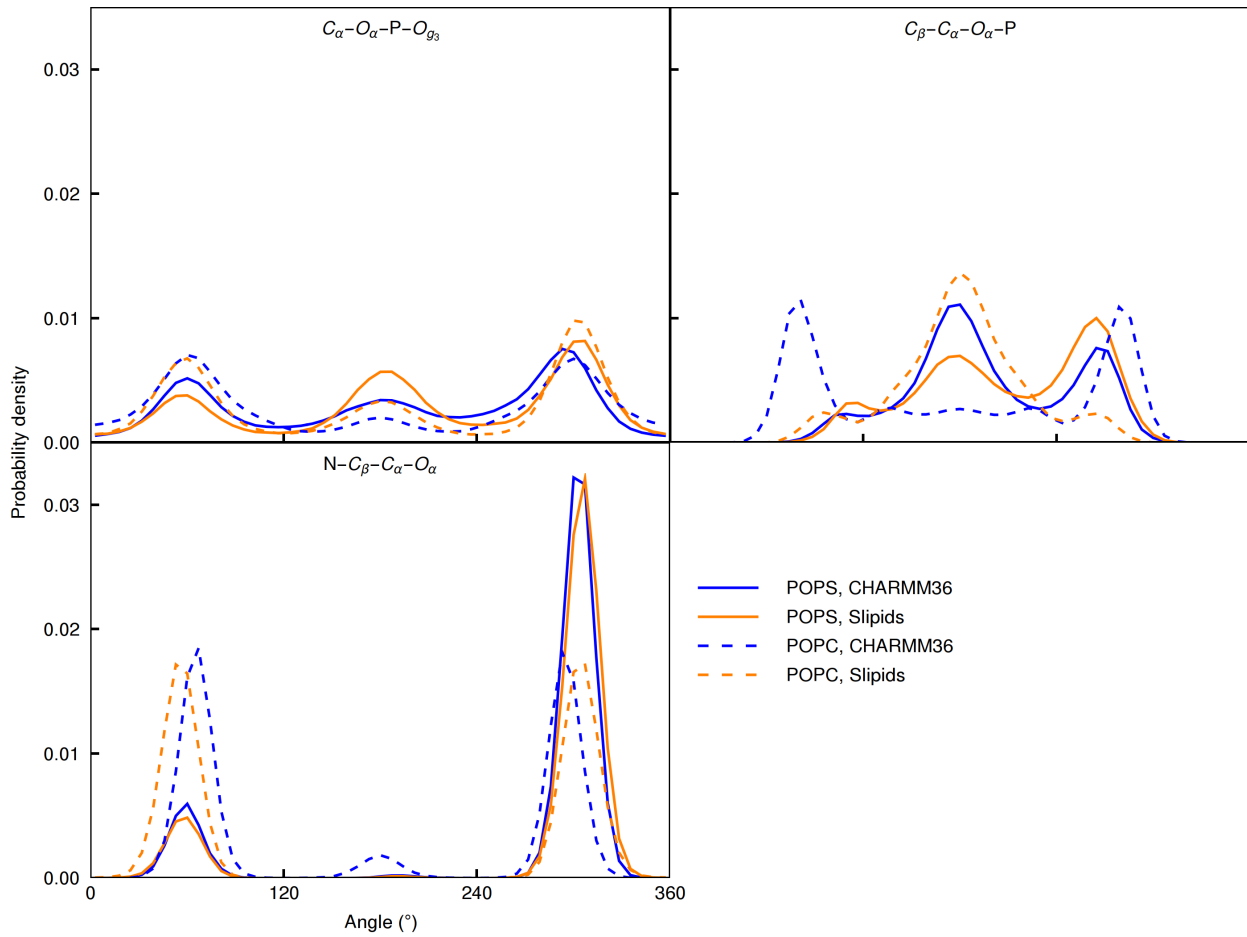


Figure S10: Dihedral angle distributions in the headgroup region from CHARMM36 and Slipids simulations compared between the POPC and POPS lipids. The CHARMM36 POPC simulation is from Ref. 100 and Slipids POPC from Ref. 101.

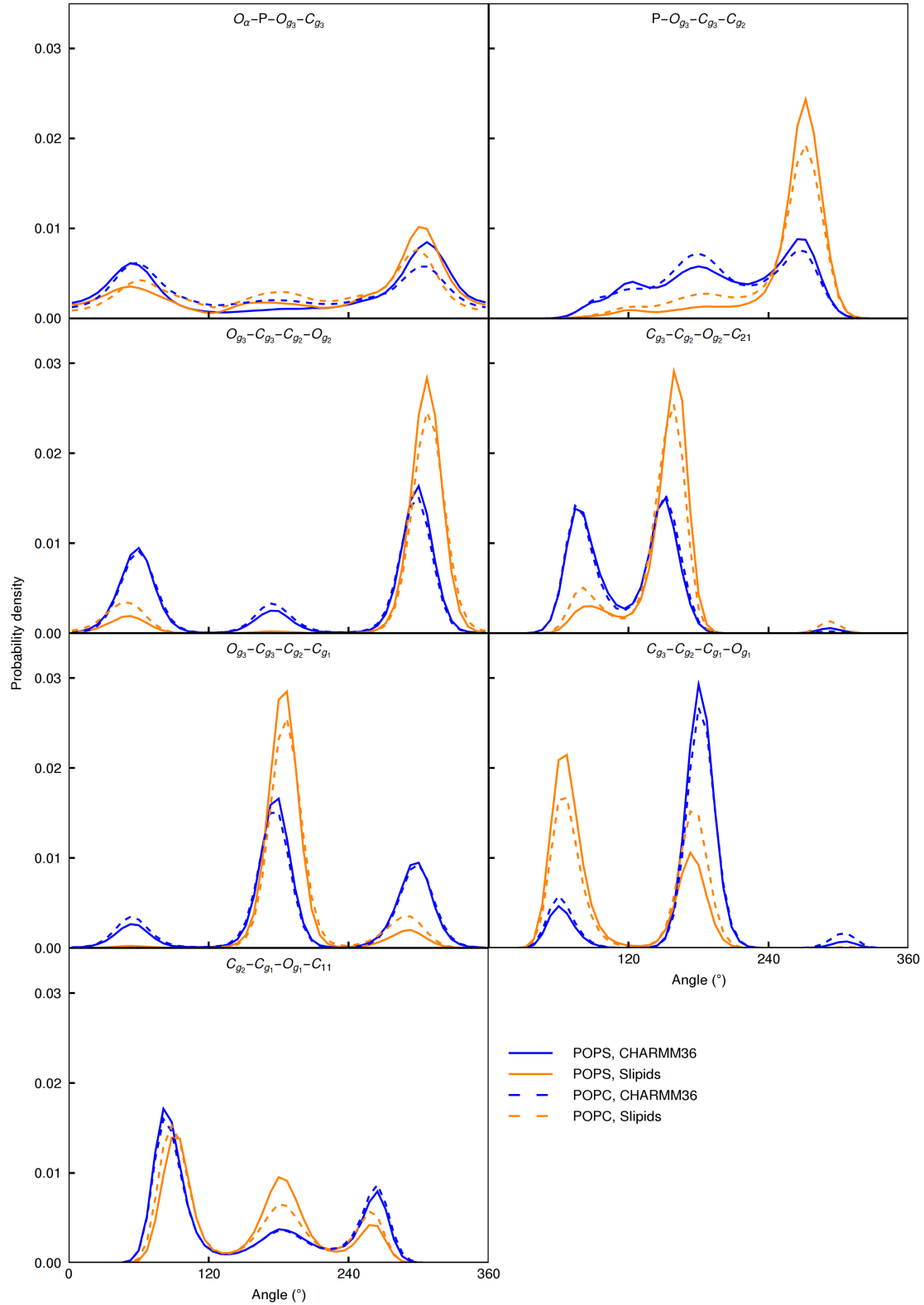


Figure S11: Dihedral angle distributions in the glycerol backbone region from CHARMM36 and Slipids simulations compared between the POPC and POPS lipids. The CHARMM36 POPC simulation is from Ref. 100 and Slipids POPC from Ref. 101.

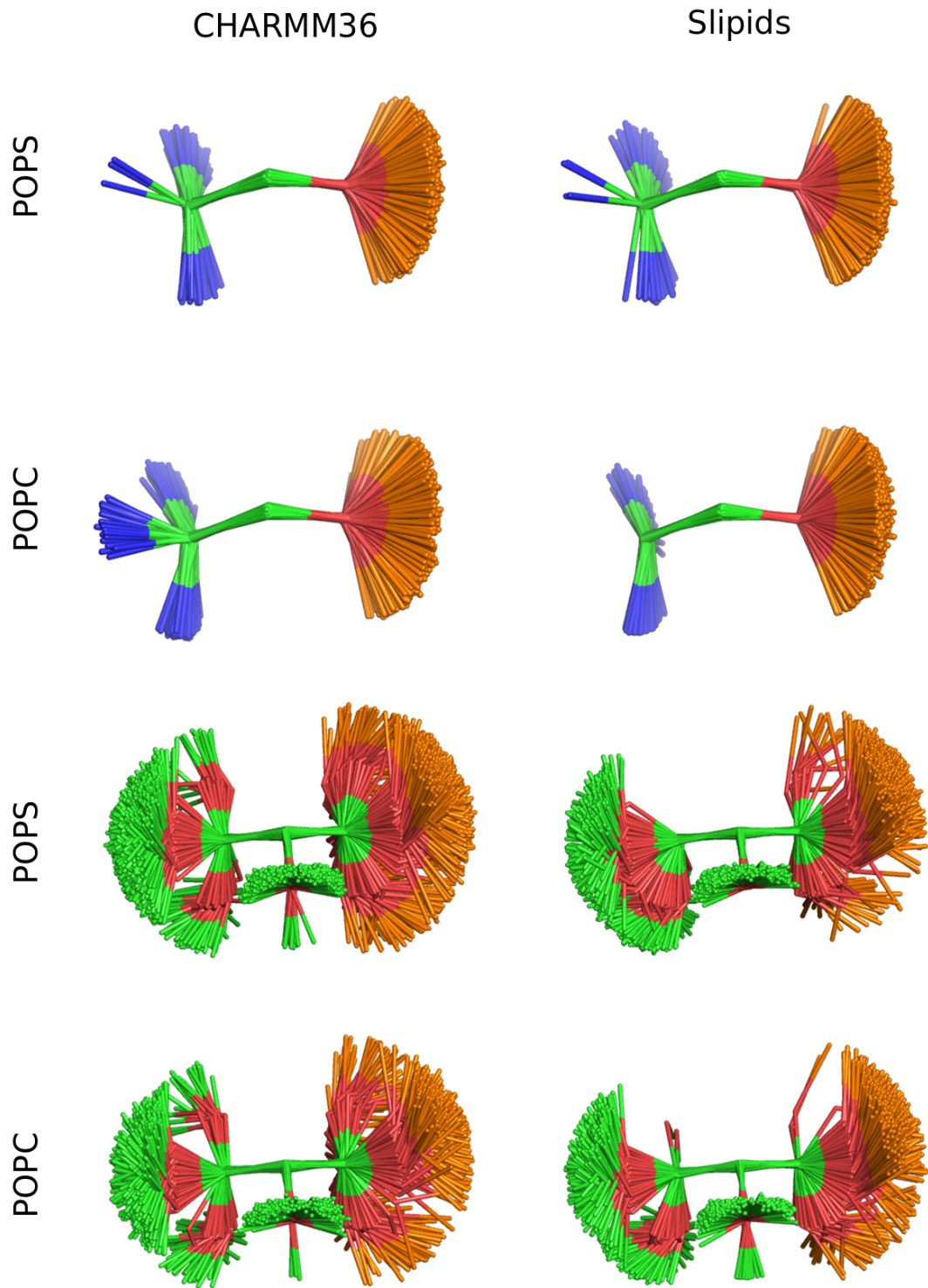


Figure S12: Overlayed snapshots of the headgroup and glycerol backbone regions from CHARMM36 and Slipids simulations compared between the POPC and POPS lipids. The CHARMM36 POPC simulation is from Ref. 100 and Slipids POPC from Ref. 101.

S7 Headgroup response to additional counterions in POPC:POPS (5:1) mixtures

To evaluate counterion binding in different simulation models against experimental data,¹⁶ Fig. S13 plots the headgroup order parameters S_{CH}^{β} and S_{CH}^{α} measured from a POPC:POPS (5:1) mixture as a function of different monovalent ions added to the buffer. Experimental order parameters of the POPC headgroup in the mixture are available as a function of LiCl and KCl concentrations, while the POPS headgroup order parameters are measured also with increasing NaCl concentration. Lithium interacts more strongly with PS headgroups than other monovalent ions,^{16,89,102–104} as also observed for PC headgroups.¹⁰⁵ The different binding behavior is evident in the responses of the PS headgroup order parameters, as for example the larger S_{CH}^{α} decreases with Li^+ , but increases with K^+ and Na^+ , see Fig. S13. The PC headgroup order parameters exhibit a clear decrease as a function of LiCl concentration but only modest changes as a function of KCl concentration, indicating significant Li^+ binding, but only weak K^+ binding, when interpreted using the molecular electrometer concept.^{83–85}

In simulations with Berger and CHARMM36, the responses of POPC and POPS S_{CH} to added sodium and potassium are not in line with the experiments. Rather, the simulations produce responses similar to experiments conducted in LiCl (Fig. S13), indicating overestimated binding affinity of sodium and potassium in these simulations. The MacRog simulations with potassium exhibit weaker counterion binding affinity (Fig. S14), but significantly larger error bars and less systematic changes in the order parameters (Fig. S13). Similar unsystematic behavior was also observed in the simulations of Lipid14/17 model with the additional counterions,^{30–33} for which the data are not shown due to the formation of ion clusters in water at relatively low (1 M) ion concentrations (Fig. S15). Appearance of such clusters in the MagRog simulations at 4 M KCl could explain the unsystematic changes of the order parameters in this model upon increasing KCl. In conclusion, the results are in line with the section 'Counterion binding and interactions between PC and PS headgroups'

in the main text, suggesting that the MacRog simulations with KCl gave the most realistic surface charge at the POPC:POPS (5:1) lipid bilayer interface among the tested simulation models.

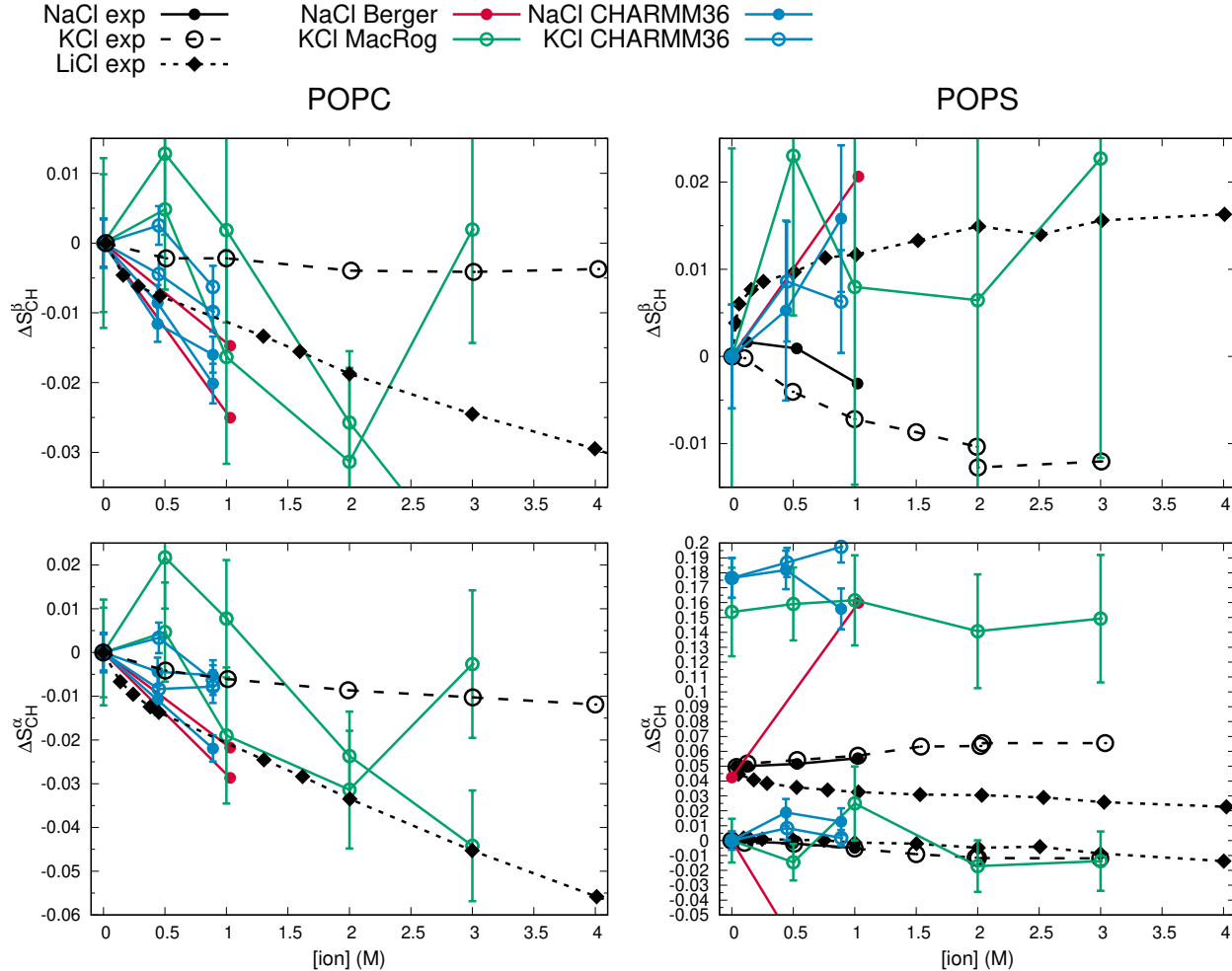


Figure S13: Changes of the PC (left) and PS (right) headgroup order parameters as a function of added NaCl, KCl and LiCl from POPC:POPS (5:1) mixture at 298 K (except Berger simulations are (4:1) mixture at 310 K). The experimental data is from Ref. 16. The values from counterion-only systems are set as a zero point of y-axis. To correctly illustrate the significant forking of the α -carbon order parameter in the PS headgroup (bottom right), the y-axis is shifted with the same value for both S_{CH}^{α} such that the lower order parameter value is at zero.

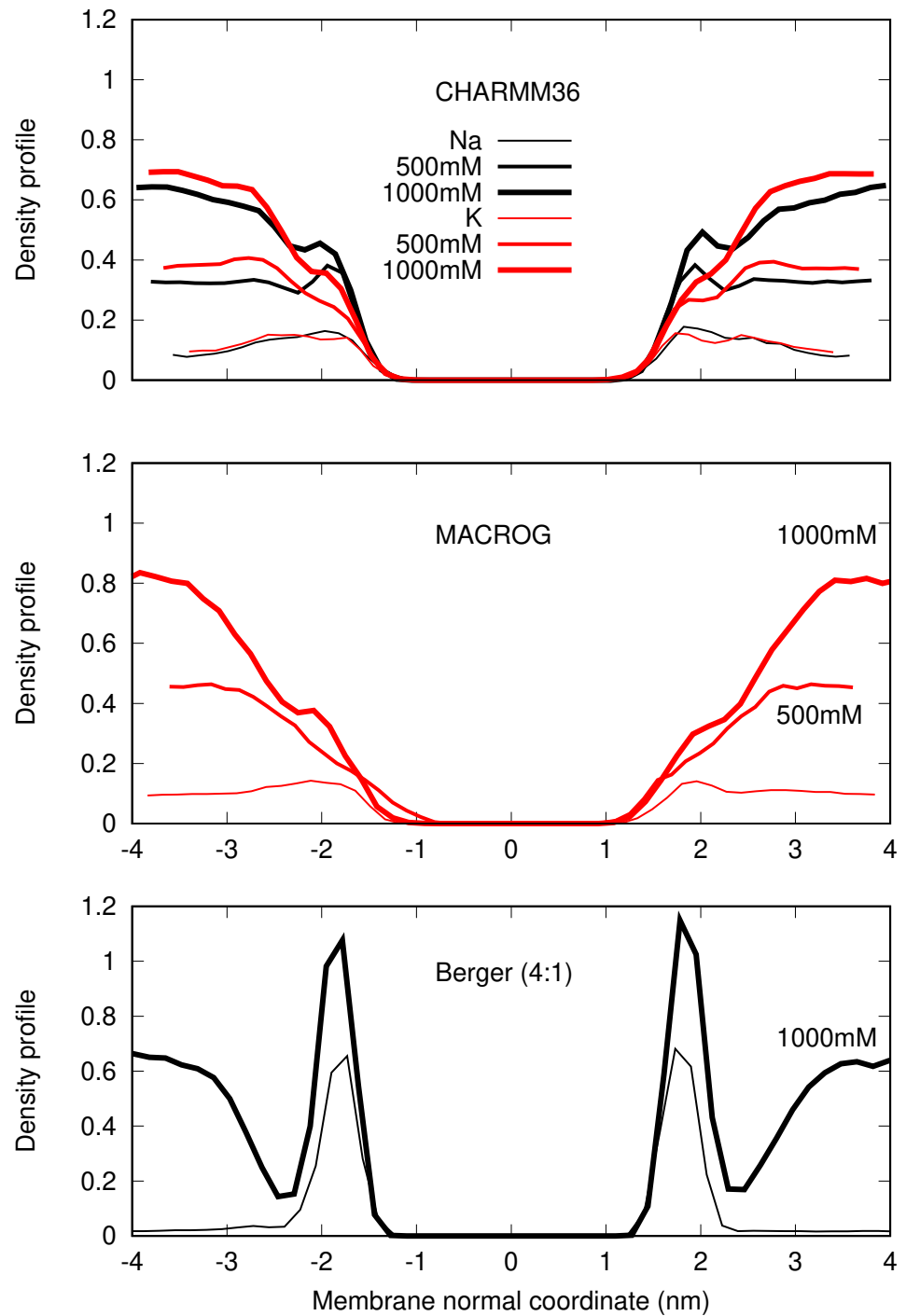


Figure S14: Counterion density distributions from PC:PS mixtures.

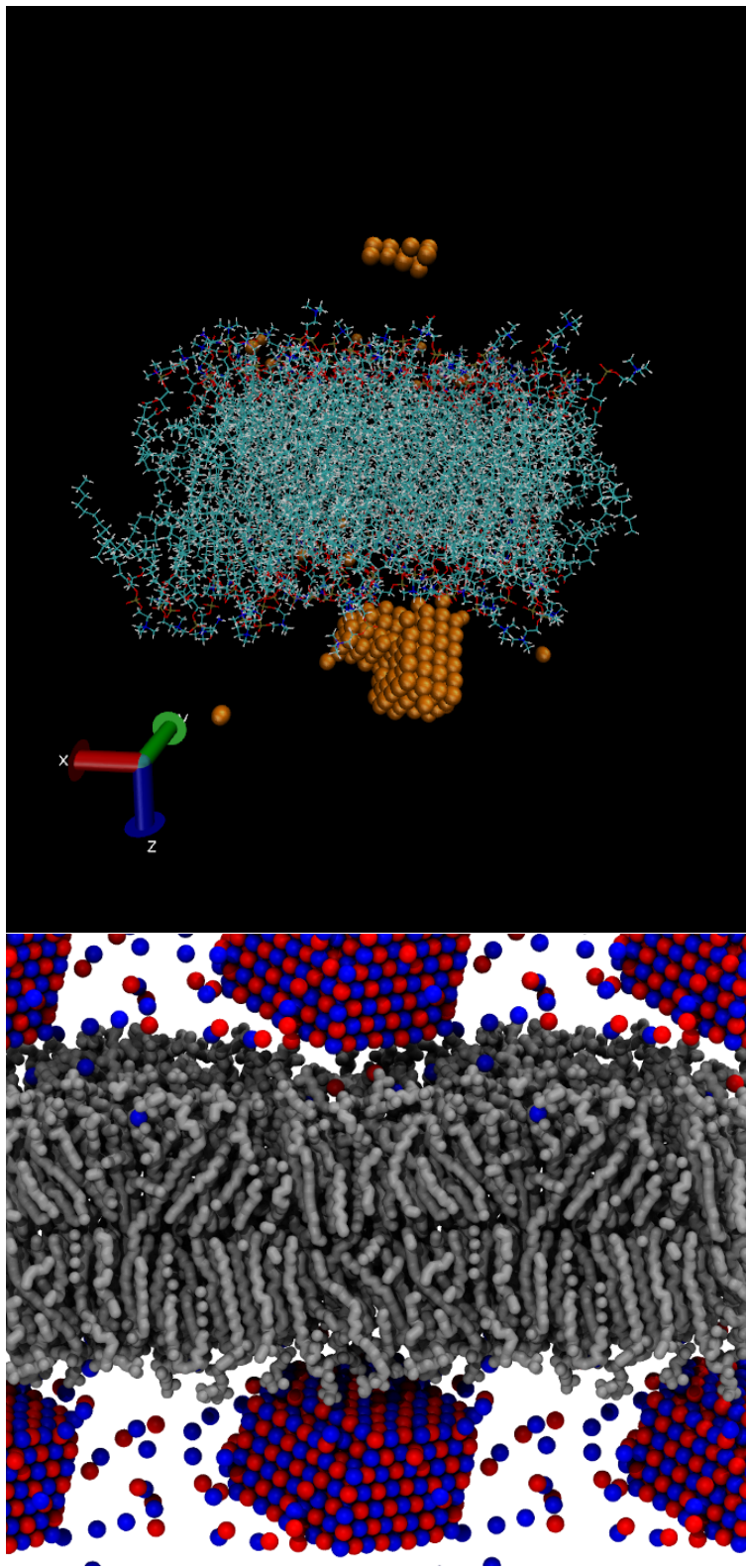


Figure S15: Ion clusters appearing in POPC:POPS (5:1) Lipid14/17 simulations with 1 M of NaCl (top) and MacRog simulations with 4 M of KCl (bottom).

S8 Calcium binding to POPC in CHARMM36 with NBfix1 parameters

The response of POPC headgroup order parameters to CaCl_2 concentration are underestimated in simulations of POPC:POPS (5:1) mixture with CHARMM36 when employing the NBfix parameters for the interactions between calcium and lipid oxygens^{38,39} (Fig. 9 in the main text), indicating that calcium binding to the bilayer is too weak with these parameters. With the NBfix1 parameters³⁸ the response of headgroup order parameters (Fig. S16) and the binding affinity of calcium (Fig. S17) were underestimated also in simulations of pure POPC bilayer. Notably, CHARMM36 simulations with the NBfix1 terms^{5,38} predict similar binding affinity for sodium and calcium. Because the results for POPC:POPS (5:1) mixture were very similar with both NBfix parameters,^{38,39} the NBfix2 parameters were not separately tested with pure POPC bilayers. Without the NBfix parameters, the calcium binding affinity to pure POPC lipid bilayers was overestimated in the CHARMM36 model.⁹⁵

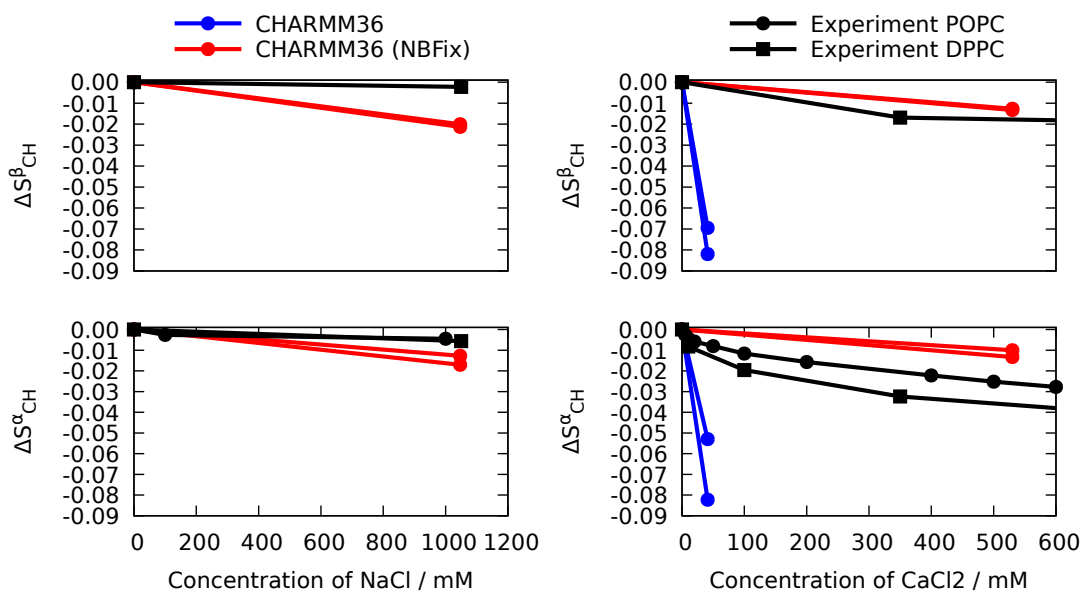


Figure S16: Headgroup order parameters from CHARMM36 simulations of POPC, where the NBfix term was employed for sodium⁵ (left) and calcium³⁸ (right), compared with the experimental data^{83,84} and simulations without NBfix for calcium. Simulation files without ions are available at Ref. 106, with the NBfix term in sodium at Ref. 107, with the NBfix term in calcium at Ref. 108, and without the NBfix in calcium at Ref. 109.

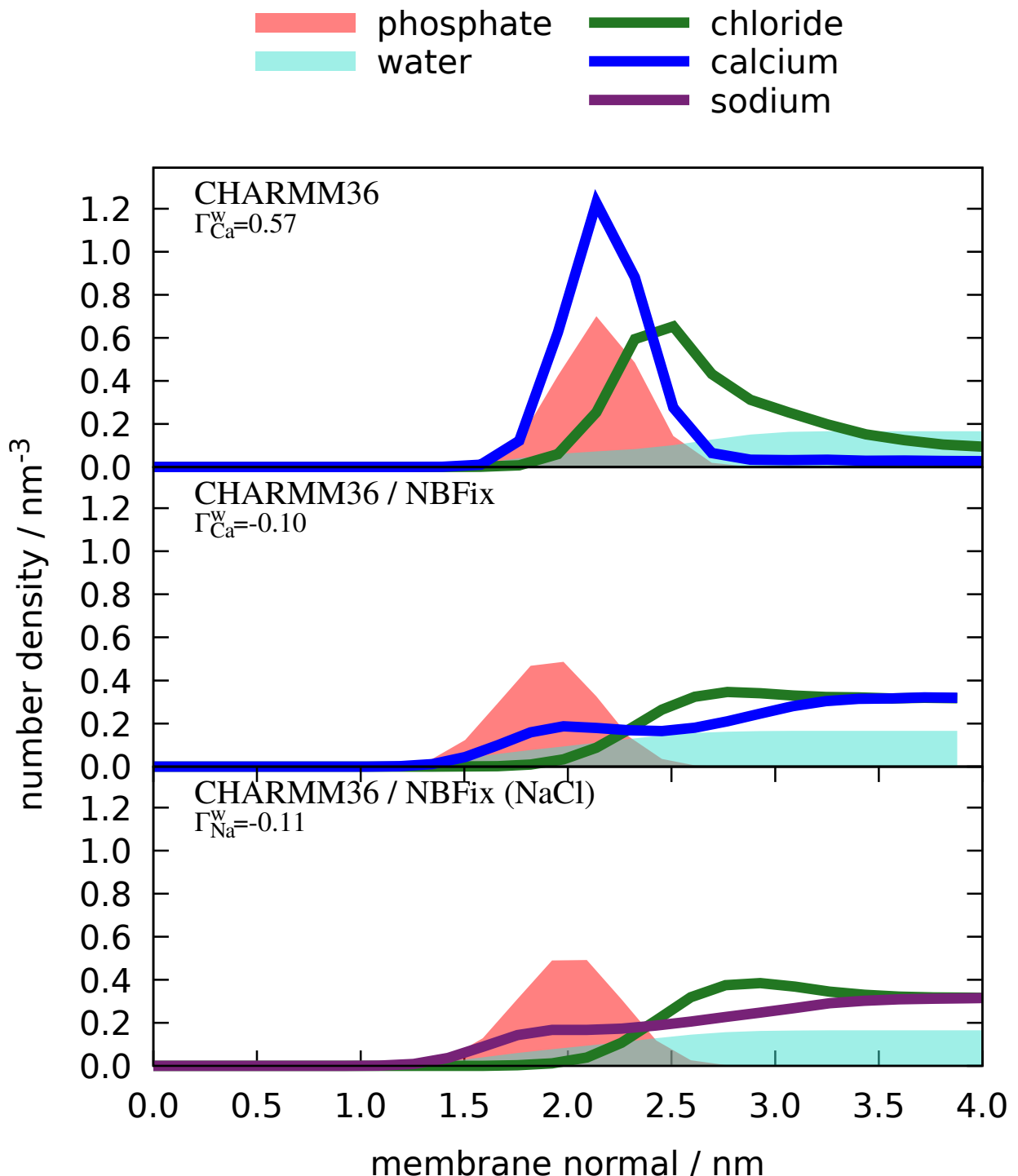


Figure S17: Density profiles along membrane normal from CHARMM36 simulations with (middle) and without (top) the NBfix term for calcium³⁸ compared to the simulation with the NBfix term for sodium⁵ (bottom). The simulation data are the same as in Fig. S16.

S9 Calcium density profiles from simulations with POPC:POPS (5:1) mixture

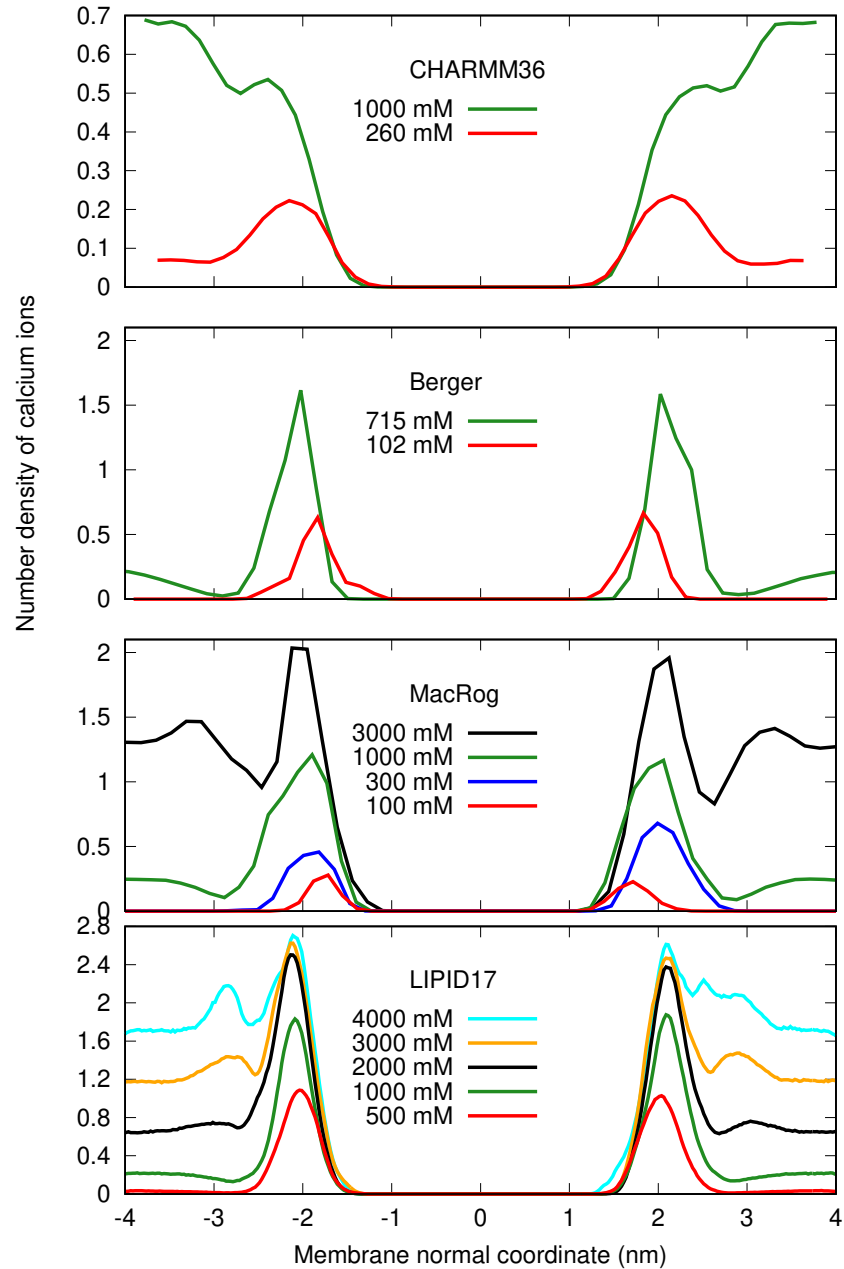


Figure S18: Number density profiles of Ca^{2+} from POPC:POPS (5:1) mixtures simulated with different force fields. The ion densities are taken along the z -axis that coincides with the bilayer normal, $z = 0$ indicating the bilayer center.

S10 Details of the force field ranking (Fig. 4)

In Fig. 4 of main text we present a rough and subjective ranking of the force fields investigated in this work. The assessment was based on the data presented in Fig. 3. For each carbon (the columns in Fig. 3), we first investigated separately how well a given force field represents the **magnitude** of the order parameters and their **forking**.

Magnitude

To quantify how close the experimentally obtained C–H order parameters were to the S_{CHS} obtained from the different MD models, we assigned a number for each carbon based on the following 5-step scale:

0 (): More than half of all the calculated S_{CHS} (includes all hydrogens bound to that carbon and all lipid tail types investigated for the given force field) were within the *subjective sweet spots* (SSP, blue-shaded areas in Fig. 3).

1 (m): All the calculated S_{CHS} were < 0.03 units away from the SSP.

2 (M): All the calculated S_{CHS} were < 0.05 units away from the SSP.

3 (M): All the calculated S_{CHS} were < 0.10 units away from the SSP.

4 (M): Some of the calculated S_{CHS} were > 0.10 units away from the SSP.

Forking

Forking in each force field was assessed based on how well the difference in order parameters of two hydrogens attached to a given carbon matched that obtained experimentally. Note that this is not relevant for β and g_2 , which have only one hydrogen. For the α carbon, for which a considerable forking of 0.105 is experimentally seen, the following 5-step scale was used:

0 (): The distance D between the symbols (indicating time-weighted averages in Fig. 3) was $0.08 < D < 0.13$ units for all the calculated S_{CHS} (includes all lipid tail types investigated for a given force field).

1 (F): $(0.06 < D < 0.08)$ OR $(0.13 < D < 0.15)$.

2 (F): $(0.04 < D < 0.06)$ OR $(0.15 < D < 0.17)$.

3 (F): $(0.02 < D < 0.04)$ OR $(0.17 < D < 0.19)$.

4 (F): $(D < 0.02)$ OR $(0.19 < D)$.

For the g_3 carbon, for which no forking is indicated by experiments, the following 5-step scale was employed:

0 (): $D < 0.02$.

1 (F): $0.02 < D < 0.04$.

2 (F): $0.04 < D < 0.06$.

3 (F): $0.06 < D < 0.08$.

4 (F): $0.08 < D$.

For the g_1 carbon, for which a considerable forking of 0.13 is experimentally seen, the following 5-step scale was utilized:

0 (): $0.11 < D < 0.15$.

1 (F): $(0.09 < D < 0.11)$ OR $(0.15 < D < 0.17)$.

2 (F): $(0.07 < D < 0.09)$ OR $(0.17 < D < 0.19)$.

3 (F): $(0.05 < D < 0.07)$ OR $(0.19 < D < 0.21)$.

4 (F): $(D < 0.05)$ OR $(0.21 < D)$.

Based on these assessments of magnitude and forking deviations from experimental values, each carbon was then assigned to one of the following groups: "within experimental error" (magnitude and forking deviations both on 0 of the scales described above), "almost within experimental error" (sum of the magnitude and forking deviation 1 or 2), "clear deviation from experiments" (sum of magnitude and forking deviation from 3 to 5), and "major deviation from experiments" (sum of magnitude and forking deviation from 6 to 8). These groups are indicated by colors in Fig. 4. (Note that for β and g_2 , for which there can be no forking, the corresponding group assignment limits were: 0, 1, 2, and 3.)

Finally, the total ability of the force field to describe the headgroup and glycerol structure was estimated. To this end, the groups were given the following weights: 0 (within experimental error), 1 (almost within experimental error), 2 (clear deviation from experiments), 4 (major deviation from experiments), and the contributions from the five carbons were summed up. The sum, given in the Σ -column of Fig. 4, was then used to (roughly and subjectively) rank the force fields.

S11 Author contributions

Hanne Antila contributed to the development of analysis tools used for evaluating the force fields, provided critical discussion on the manuscript content, and edited it for clarity.

Pavel Buslaev analysed the dihedral angle distributions in the head group and glycerol backbone regions.

Fernando Favela-Rosales set up and performed one of the DOPS simulations with Slipids.

Tiago M. Ferreira performed the NMR experiments and NMR simulations, processed and analysed the experimental data, prepared the corresponding figures, wrote parts of the manuscript (NMR methods and interpretation of the S-DROSS results), and took part in the final revision.

Ivan Gushchin supervised the work of P.B.

Matti Javanainen performed most of the MacRog simulations, and provided comments on the manuscript.

Batuhan Kav set up, performed, and analysed Amber Lipid14/17 simulations with the Amber MD simulation package.

Jesper J. Madsen set up, performed, and analysed several of the CHARMM36 simulations. Provided comments on the manuscript.

Josef Melcr prepared tools for calculating order parameters, performed Lipid14/17 simulations with Gromacs MD simulation package, and provided comments on the manuscript.

Markus S. Miettinen worked with H. A. on the analysis tools, and with B. K. on the Amber MD simulations. Made the subjective force field ranking. Edited the manuscript.

Jukka Määttä prepared figures 6 and 10.

Ricky Nencini ran the simulations of POPC systems using CHARMM36 with and without the NBfix corrections, ran the simulations of POPC:POPS (5:1) systems using CHARMM36 with the NBfix2 correction, and analyzed the difference between bulk and buffer concentrations.

O. H. Samuli Ollila designed the project and managed the work. Ran and analysed several simulations. Wrote the manuscript.

Thomas J. Piggot set up, performed, and analysed many of the simulations. Contributed to parts of the manuscript.

References

- (1) Botan, A.; Favela-Rosales, F.; Fuchs, P. F. J.; Javanainen, M.; Kanduč, M.; Kulig, W.; Lamberg, A.; Loison, C.; Lyubartsev, A.; Miettinen, M. S. et al. Toward Atomistic Resolution Structure of Phosphatidylcholine Headgroup and Glycerol Backbone at Different Ambient Conditions. *J. Phys. Chem. B* **2015**, *119*, 15075–15088.
- (2) Fernando, F.-R. POPC_Glycerol_CHARMM36_0-10-15-20-25-35-50%CHOL. 2015; <http://dx.doi.org/10.5281/zenodo.16830>, Because of the system size, the files ONLY contain the coordinates of Glycerol saved every 10ps, this is the real contribution to the nmrlipids project.
- (3) Lee, J.; Cheng, X.; Swails, J. M.; Yeom, M. S.; Eastman, P. K.; Lemkul, J. A.; Wei, S.; Buckner, J.; Jeong, J. C.; Qi, Y. et al. CHARMM-GUI Input Generator for NAMD, GROMACS, AMBER, OpenMM, and CHARMM/OpenMM Simulations Using the CHARMM36 Additive Force Field. *J. Chem. Theory Comput.* **2016**, *12*, 405–413.
- (4) Jo, S.; Kim, T.; Iyer, V. G.; Im, W. CHARMM-GUI: A Web-Based Graphical User Interface for CHARMM. *J. Comput. Chem.* **29**, 1859–1865.
- (5) Venable, R. M.; Luo, Y.; Gawrisch, K.; Roux, B.; Pastor, R. W. Simulations of Anionic Lipid Membranes: Development of Interaction-Specific Ion Parameters and Validation Using NMR Data. *J. Phys. Chem. B* **2013**, *117*, 10183–10192.
- (6) Durell, S. R.; Brooks, B. R.; Ben-Naim, A. Solvent-Induced Forces Between Two Hydrophilic Groups. *The Journal of Physical Chemistry* **1994**, *98*, 2198–2202.
- (7) Neria, E.; Fischer, S.; Karplus, M. Simulation of Activation Free Energies in Molecular Systems. *J. Chem. Phys.* **1996**, *105*, 1902–1921.
- (8) Abraham, M. J.; Murtola, T.; Schulz, R.; Páll, S.; Smith, J. C.; Hess, B.; Lindahl, E.

GROMACS: High Performance Molecular Simulations Through Multi-Level Parallelism from Laptops to Supercomputers. *SoftwareX* **2015**, *1*, 19–25.

- (9) Hess, B.; Bekker, H.; Berendsen, H. J. C.; Fraaije, J. G. E. M. LINCS: a linear constraint solver for molecular dynamics simulations. *J. Comput. Chem.* **1997**, *18*, 1463–1472.
- (10) Hess, B. P-LINCS: A Parallel Linear Constraint Solver for Molecular Simulation. *J. Chem. Theory Comput.* **2008**, *4*, 116–122.
- (11) Nose, S. A molecular dynamics method for simulations in the canonical ensemble. *Mol. Phys.* **1984**, *52*, 255–268.
- (12) Hoover, W. G. Canonical dynamics: Equilibrium phase-space distributions. *Phys. Rev. A* **1985**, *31*, 1695–1697.
- (13) Parrinello, M.; Rahman, A. Polymorphic transitions in single crystals: A new molecular dynamics method. *J. Appl. Phys.* **1981**, *52*, 7182–7190.
- (14) Darden, T.; York, D.; Pedersen, L. Particle Mesh Ewald: An N·log(N) Method for Ewald Sums in Large Systems. *J. Chem. Phys.* **1993**, *98*, 10089–10092.
- (15) Essman, U. L.; Perera, M. L.; Berkowitz, M. L.; Larden, T.; Lee, H.; Pedersen, L. G. A smooth particle mesh ewald potential. *J. Chem. Phys.* **1995**, *103*, 8577–8592.
- (16) Roux, M.; Bloom, M. Calcium, Magnesium, Lithium, Sodium, and Potassium Distributions in the Headgroup Region of Binary Membranes of Phosphatidylcholine and Phosphatidylserine As Seen by Deuterium NMR. *Biochemistry* **1990**, *29*, 7077–7089.
- (17) Klauda, J. B.; Venable, R. M.; Freites, J. A.; O'Connor, J. W.; Tobias, D. J.; Mondragon-Ramirez, C.; Vorobyov, I.; MacKerell Jr, A. D.; Pastor, R. W. Update of the CHARMM All-Atom Additive Force Field for Lipids: Validation on Six Lipid Types. *J. Phys. Chem. B* **2010**, *114*, 7830–7843.

- (18) Madsen, J. J. MD Simulations of Bilayers Containing PC/PS Mixtures and CaCl₂: 250POPC_50POPS_neutral. 2019; <https://doi.org/10.5281/zenodo.2542151>.
- (19) Piggot, T. CHARMM36 POPS/POPC Simulations (versions 1 and 2) 298 K 1.0 nm LJ Switching with K Ions. 2018; <https://doi.org/10.5281/zenodo.1182658>.
- (20) Ollila, O. H. S. POPC:POPS (5:1) with 450 mM Potassium Simulation with CHARMM36 at 298K. 2018; <https://doi.org/10.5281/zenodo.1493241>.
- (21) Ollila, O. H. S. POPC:POPS (5:1) with 890 mM Potassium Simulation with CHARMM36 at 298K. 2018; <https://doi.org/10.5281/zenodo.1493246>.
- (22) Piggot, T. CHARMM36 POPS/POPC Simulations (versions 1 and 2) 298 K 1.0 nm LJ Switching with Na Ions. 2018; <https://doi.org/10.5281/zenodo.1182665>.
- (23) Ollila, O. H. S. POPC:POPS (5:1) with 440 mM Sodium Simulation with CHARMM36 at 298K. 2018; <https://doi.org/10.5281/zenodo.1493190>.
- (24) Ollila, O. H. S. POPC:POPS (5:1) with 890 mM Sodium Simulation with CHARMM36 at 298K. 2018; <https://doi.org/10.5281/zenodo.1493229>.
- (25) Maciejewski, A.; Pasenkiewicz-Gierula, M.; Cramariuc, O.; Vattulainen, I.; Rög, T. Refined OPLS All-Atom Force Field for Saturated Phosphatidylcholine Bilayers at Full Hydration. *J. Phys. Chem. B* **2014**, *118*, 4571–4581.
- (26) Javanainen, M. Simulations of POPC/POPS Membranes with CaCl₂. 2017; <https://doi.org/10.5281/zenodo.1409551>.
- (27) Javanainen, M. Simulations of POPC/POPS Membranes with KCl. 2018; <https://doi.org/10.5281/zenodo.1404040>.
- (28) Dickson, C. J.; Madej, B. D.; Skjevik, A. A.; Betz, R. M.; Teigen, K.; Gould, I. R.; Walker, R. C. Lipid14: The Amber Lipid Force Field. *J. Chem. Theory Comput.* **2014**, *10*, 865–879.

- (29) Gould, I.; Skjevik, A.; Dickson, C.; Madej, B.; Walker, R. Lipid17: A Comprehensive AMBER Force Field for the Simulation of Zwitterionic and Anionic Lipids. 2018; In preparation.
- (30) Kav, B.; Miettinen, M. S. Amber Lipid17 Simulations of POPC/POPS Membranes with KCl Counterions. 2018; <https://doi.org/10.5281/zenodo.1250969>.
- (31) Kav, B.; Miettinen, M. S. Amber Lipid17 Simulations of POPC/POPS Membranes with KCl. 2018; <https://doi.org/10.5281/zenodo.1227257>.
- (32) Kav, B.; Miettinen, M. S. Amber Lipid17 Simulations of POPC/POPS Membranes with NaCl Counterions. 2018; <https://doi.org/10.5281/zenodo.1250975>.
- (33) Kav, B.; Miettinen, M. S. Amber Lipid17 Simulations of POPC/POPS Membranes with NaCl. 2018; <https://doi.org/10.5281/zenodo.1227272>.
- (34) Tieleman, D. P.; Berendsen, H. J.; Sansom, M. S. an Alamethicin Channel in a Lipid Bilayer: Molecular Dynamics Simulations. *Biophys. J.* **1999**, *76*, 1757 – 1769.
- (35) Mukhopadhyay, P.; Monticelli, L.; Tieleman, D. P. Molecular Dynamics Simulation of a Palmitoyl-Oleoyl Phosphatidylserine Bilayer with Na⁺ Counterions and NaCl. *Biophys. J.* **2004**, *86*, 1601 – 1609.
- (36) Ollila, O. H. S. POPC:POPS (4:1) Simulation with Berger Model at 310K. 2018; <https://doi.org/10.5281/zenodo.1475285>.
- (37) Cwiklik, L. MD Simulation Trajectory of a POPC/POPS (4:1) Bilayer with 1M NaCl, Berger Force Field for Lipids and Ffgmx for Ions. 2017; <https://doi.org/10.5281/zenodo.838219>.
- (38) Kim, S.; Patel, D. S.; Park, S.; Slusky, J.; Klauda, J. B.; Widmalm, G.; Im, W. Bilayer Properties of Lipid a from Various Gram-Negative Bacteria. *Biophys. J.* **2016**, *111*, 1750 – 1760.

- (39) Han, K.; Venable, R. M.; Bryant, A.-M.; Legacy, C. J.; Shen, R.; Li, H.; Roux, B.; Gericke, A.; Pastor, R. W. Graph-Theoretic Analysis of Monomethyl Phosphate Clustering in Ionic Solutions. *The Journal of Physical Chemistry B* **2018**, *122*, 1484–1494.
- (40) Lee, S.; Tran, A.; Allsopp, M.; Lim, J. B.; Henin, J.; Klauda, J. B. CHARMM36 United Atom Chain Model for Lipids and Surfactants. *J. Phys. Chem. B* **2014**, *118*, 547–556.
- (41) Kulig, W.; Pasenkiewicz-Gierula, M.; Róg, T. Topologies, Structures and Parameter Files for Lipid Simulations in GROMACS with the OPLS-Aa Force Field: DPPC, POPC, DOPC, PEPC, and Cholesterol. *Data in Brief* **2015**, *5*, 333 – 336.
- (42) Kulig, W.; Pasenkiewicz-Gierula, M.; Róg, T. Cis and Trans Unsaturated Phosphatidyl-choline Bilayers: A Molecular Dynamics Simulation Study. *Chem. Phys. Lipids* **2016**, *195*, 12 – 20.
- (43) Jorgensen, W. L.; Chandrasekhar, J.; Madura, J. D.; Impey, R. W.; Klein, M. L. Comparison of Simple Potential Functions for Simulating Liquid Water. *J. Chem. Phys.* **1983**, *79*, 926–935.
- (44) Javanainen, M. Simulation of a POPC Bilayer at 298K, Lipid Model by Maciejewski and Rog. 2018; <https://doi.org/10.5281/zenodo.1167532>.
- (45) Róg, T.; Orłowski, A.; Llorente, A.; Skotland, T.; Sylvänen, T.; Kauhanen, D.; Ekroos, K.; Sandvig, K.; Vattulainen, I. Data Including GROMACS Input Files for Atomistic Molecular Dynamics Simulations of Mixed, Asymmetric Bilayers Including Molecular Topologies, Equilibrated Structures, and Force Field for Lipids Compatible with OPLS-Aa Parameters. *Data in Brief* **2016**, *7*, 1171 – 1174.
- (46) Javanainen, M. Simulation of a POPS Membrane with Potassium Counterions. 2018; <https://doi.org/10.5281/zenodo.1434990>.

- (47) Páll, S.; Hess, B. A Flexible Algorithm for Calculating Pair Interactions on SIMD Architectures. *Comput. Phys. Commun.* **2013**, *184*, 2641 – 2650.
- (48) Åqvist, J. Ion-Water Interaction Potentials Derived from Free Energy Perturbation Simulations. *J. Phys. Chem.* **1990**, *94*, 8021–8024.
- (49) Shirts, M. R.; Mobley, D. L.; Chodera, J. D.; Pande, V. S. Accurate and Efficient Corrections for Missing Dispersion Interactions in Molecular Simulations. *J. Phys. Chem. B* **2007**, *111*, 13052–13063.
- (50) Miyamoto, S.; Kollman, P. A. SETTLE: An analytical Version of the SHAKE and RATTLE Algorithm for Rigid Water Models. *J. Comput. Chem* **1992**, *13*, 952–962.
- (51) Jorgensen, W. L.; Chandrasekhar, J.; Madura, J. D.; Impey, R. W.; Klein, M. L. Comparison of Simple Potential Functions for Simulating Liquid Water. *The Journal of chemical physics* **1983**, *79*, 926–935.
- (52) Case, D.; Ben-Shalom, I.; Brozell, S.; Cerutti, D.; III, T. C.; Cruzeiro, V.; Darden, T.; Duke, R.; Ghoreishi, D.; Gilson, M. et al. AMBER 2018. 2018.
- (53) Joung, I. S.; Cheatham III, T. E. Determination of Alkali and Halide Monovalent Ion Parameters for Use in Explicitly Solvated Biomolecular Simulations. *The journal of physical chemistry B* **2008**, *112*, 9020–9041.
- (54) Miettinen, M. S.; Kav, B. Molecular Dynamics Simulation Trajectory of an Anionic Lipid Bilayer: 100 Mol% POPC with Na⁺ Counterions Using Joung-Cheatham Ions. 2018; <https://doi.org/10.5281/zenodo.1148495>.
- (55) Miettinen, M. S.; Kav, B. Molecular Dynamics Simulation Trajectory of an Anionic Lipid Bilayer: 100 Mol% POPC with Na⁺ Counterions Using Ff99 Ions. 2018; <https://doi.org/10.5281/zenodo.1134869>.

- (56) Kav, B.; Miettinen, M. S. Molecular Dynamics Simulation Trajectory of an Anionic Lipid Bilayer: 100 Mol% DOPS with Na+ Counterions Using Joung-Cheetham Ions. 2018; <https://doi.org/10.5281/zenodo.1134871>.
- (57) Kav, B.; Miettinen, M. S. Molecular Dynamics Simulation Trajectory of an Anionic Lipid Bilayer: 100 Mol% DOPS with Na+ Counterions Using Ff99 Ions. 2018; <https://doi.org/10.5281/zenodo.1135142>.
- (58) Kav, B.; Miettinen, M. S. Amber Lipid17 Simulations of POPC/POPS Membranes with CaCl₂. 2018; <https://doi.org/10.5281/zenodo.1438848>.
- (59) Sousa da Silva, A.; Vranken, W. ACPYPE - AnteChamber PYthon Parser interfacE. *BMC Research Notes* **2012**, *5*, 367.
- (60) Ollila, O. H. S.; Retegan, M. MD Simulation Trajectory and Related Files for POPC Bilayer (Lipid14, Gromacs 4.5). 2014; <http://dx.doi.org/10.5281/zenodo.12767>.
- (61) Smith, D. E.; Dang, L. X. Computer Simulations of NaCl Association in Polarizable Water. *J. Chem. Phys* **1994**, *100*, 3757–3766.
- (62) Dang, L. X.; Schenter, G. K.; Glezakou, V.-A.; Fulton, J. L. Molecular Simulation Analysis and X-Ray Absorption Measurement of Ca²⁺, K⁺ and Cl⁻ Ions in Solution. *J. Phys. Chem. B* **2006**, *110*, 23644–54.
- (63) Bussi, G.; Donadio, D.; Parrinello, M. Canonical Sampling Through Velocity Rescaling. *J. Chem. Phys.* **2007**, *126*.
- (64) Melcr, J. Molecular Dynamics Simulations of Lipid Bilayers Containing POPC and POPS with the Lipid17 Force Field, Only Counterions, and CaCl₂ Concentrations. 2018; <https://doi.org/10.5281/zenodo.1487761>.
- (65) Melcr, J.; Ferreira, T.; Jungwirth, P.; Ollila, O. H. S. Improved Cation Binding to Lipid Bilayer with Negatively Charged POPS by Effective Inclu-

sion of Electronic Polarization. https://github.com/ohsOllila/ecc_lipids/blob/master/Manuscript/manuscript.pdf, Submitted.

- (66) Jämbeck, J. P. M.; Lyubartsev, A. P. Implicit Inclusion of Atomic Polarization in Modeling of Partitioning Between Water and Lipid Bilayers. *Phys. Chem. Chem. Phys.* **2013**, *15*, 4677–4686.
- (67) Jämbeck, J. P.; Lyubartsev, A. P. Another Piece of the Membrane Puzzle: Extending Slipids Further. *Journal of chemical theory and computation* **2012**, *9*, 774–784.
- (68) Wennberg, C. L.; Murtola, T.; PÅall, S.; Abraham, M. J.; Hess, B.; Lindahl, E. Direct-Space Corrections Enable Fast and Accurate Lorentz–Berthelot Combination Rule Lennard-Jones Lattice Summation. *J. Chem. Theory Comput.* **2015**, *11*, 5737–5746.
- (69) Ghahremanpour, M. M.; Arab, S. S.; Aghazadeh, S. B.; Zhang, J.; van der Spoel, D. MemBuilder: A Web-Based Graphical Interface to Build Heterogeneously Mixed Membrane Bilayers for the GROMACS Biomolecular Simulation Program. *Bioinformatics* **2013**, *30*, 439–441.
- (70) Ollila, S.; Hyvönen, M. T.; Vattulainen, I. Polyunsaturation in Lipid Membranes: Dynamic Properties and Lateral Pressure Profiles. *J. Phys. Chem. B* **2007**, *111*, 3139–3150.
- (71) Ollila, O. H. S. MD Simulation of POPC Lipids Bilayer at 310K (Berger, Gromacs 3.1.4). 2018; <https://doi.org/10.5281/zenodo.1230170>.
- (72) Berendsen, H. J. C.; Postma, J. P. M.; van Gunsteren, W. F.; Hermans, J. In *Intermolecular Forces*; Pullman, B., Ed.; Reidel: Dordrecht, 1981; Chapter Interaction models for water in relation to protein hydration, pp 331–342.
- (73) Jurkiewicz, P.; Cwiklik, L.; Vojtíšková, A.; Jungwirth, P.; Hof, M. Structure, Dynamics,

and Hydration of POPC/POPS Bilayers Suspended in NaCl, KCl, and CsCl Solutions.

Biochim. Biophys. Acta **2012**, *1818*, 609 – 616.

- (74) Melcrová, A.; Pokorna, S.; Pullanchery, S.; Kohagen, M.; Jurkiewicz, P.; Hof, M.; Jungwirth, P.; Cremer, P. S.; Cwiklik, L. the Complex Nature of Calcium Cation Interactions with Phospholipid Bilayers. *Sci. Reports* **2016**, *6*, 38035.
- (75) Cwiklik, L. MD Simulation Trajectory of a POPC/POPS (4:1) Bilayer with 102mM CaCl₂, Berger Force Field for Lipids, Scaled Charges for Ca²⁺ and Cl⁻. 2017; <https://doi.org/10.5281/zenodo.887398>.
- (76) Cwiklik, L. MD Simulation Trajectory of a POPC/POPS (4:1) Bilayer with 715mM CaCl₂, Berger Force Field for Lipids, Scaled Charges for Ca²⁺ and Cl⁻. 2017; <https://doi.org/10.5281/zenodo.887400>.
- (77) Chandrasekhar, I.; Kastenholz, M.; Lins, R.; Oostenbrink, C.; Schuler, L.; Tieleman, D.; Gunsteren, W. A Consistent Potential Energy Parameter Set for Lipids: Dipalmitoylphosphatidylcholine As a Benchmark of the GROMOS96 45A3 Force Field. *Eur. Biophys. J.* **2003**, *32*, 67–77.
- (78) Kukol, A. Lipid Models for United-Atom Molecular Dynamics Simulations of Proteins. *J. Chem. Theory Comput.* **2009**, *5*, 615–626.
- (79) Piggot, T. J.; Piñeiro, Á.; Khalid, S. Molecular Dynamics Simulations of Phosphatidyl-choline Membranes: A Comparative Force Field Study. *J. Chem. Theory Comput.* **2012**, *8*, 4593–4609.
- (80) Piggot, T. J.; Holdbrook, D. A.; Khalid, S. Electroporation of the E. Coli and S. Aureus Membranes: Molecular Dynamics Simulations of Complex Bacterial Membranes. *J. Phys. Chem. B* **2011**, *115*, 13381–13388.

- (81) Holdbrook, D. A.; Leung, Y. M.; Piggot, T. J.; Marius, P.; Williamson, P. T. F.; Khalid, S. Stability and Membrane Orientation of the Fukutin Transmembrane Domain: A Combined Multiscale Molecular Dynamics and Circular Dichroism Study. *Biochemistry* **2010**, *49*, 10796–10802.
- (82) Schmid, N.; Eichenberger, A. P.; Choutko, A.; Riniker, S.; Winger, M.; Mark, A. E.; van Gunsteren, W. F. Definition and Testing of the GROMOS Force-Field Versions 54A7 and 54B7. *Eur. Biophys. J.* **2011**, *40*, 843.
- (83) Akutsu, H.; Seelig, J. Interaction of Metal Ions with Phosphatidylcholine Bilayer Membranes. *Biochemistry* **1981**, *20*, 7366–7373.
- (84) Altenbach, C.; Seelig, J. Calcium Binding to Phosphatidylcholine Bilayers As Studied by Deuterium Magnetic Resonance. Evidence for the Formation of a Calcium Complex with Two Phospholipid Molecules. *Biochemistry* **1984**, *23*, 3913–3920.
- (85) Seelig, J.; MacDonald, P. M.; Scherer, P. G. Phospholipid Head Groups As Sensors of Electric Charge in Membranes. *Biochemistry* **1987**, *26*, 7535–7541.
- (86) Scherer, P. G.; Seelig, J. Electric Charge Effects on Phospholipid Headgroups. Phosphatidylcholine in Mixtures with Cationic and Anionic Amphiphiles. *Biochemistry* **1989**, *28*, 7720–7728.
- (87) Borle, F.; Seelig, J. Ca²⁺ Binding to Phosphatidylglycerol Bilayers As Studied by Differential Scanning Calorimetry and ²H- and ³¹P-Nuclear Magnetic Resonance. *Chem. Phys. Lipids* **1985**, *36*, 263 – 283.
- (88) Macdonald, P. M.; Seelig, J. Calcium Binding to Mixed Phosphatidylglycerol-Phosphatidylcholine Bilayers As Studied by Deuterium Nuclear Magnetic Resonance. *Biochemistry* **1987**, *26*, 1231–1240.

- (89) Roux, M.; Neumann, J.-M. Deuterium NMR Study of Head-Group Deuterated Phosphatidylserine in Pure and Binary Phospholipid Bilayers. *FEBS Letters* **1986**, *199*, 33–38.
- (90) Roux, M.; Bloom, M. Calcium Binding by Phosphatidylserine Headgroups. Deuterium NMR Study. *Biophys. J.* **1991**, *60*, 38 – 44.
- (91) Scherer, P.; Seelig, J. Structure and Dynamics of the Phosphatidylcholine and the Phosphatidylethanolamine Head Group in L-M Fibroblasts As Studied by Deuterium Nuclear Magnetic Resonance. *EMBO J.* **1987**, *6*, 2915–2922.
- (92) Ferreira, T. M.; Coreta-Gomes, F.; Ollila, O. H. S.; Moreno, M. J.; Vaz, W. L. C.; Topgaard, D. Cholesterol and POPC Segmental Order Parameters in Lipid Membranes: Solid State ^1H - ^{13}C NMR and MD Simulation Studies. *Phys. Chem. Chem. Phys.* **2013**, *15*, 1976–1989.
- (93) Ollila, O. S.; Pabst, G. Atomistic Resolution Structure and Dynamics of Lipid Bilayers in Simulations and Experiments. *Biochim. Biophys. Acta* **2016**, *1858*, 2512 – 2528.
- (94) Ferreira, T. M.; Sood, R.; Bärenwald, R.; Carlström, G.; Topgaard, D.; Saalwächter, K.; Kinnunen, P. K. J.; Ollila, O. H. S. Acyl Chain Disorder and Azelaoyl Orientation in Lipid Membranes Containing Oxidized Lipids. *Langmuir* **2016**, *32*, 6524–6533.
- (95) Catte, A.; Girych, M.; Javanainen, M.; Loison, C.; Melcr, J.; Miettinen, M. S.; Monticelli, L.; Maatta, J.; Oganesyan, V. S.; Ollila, O. H. S. et al. Molecular Electrometer and Binding of Cations to Phospholipid Bilayers. *Phys. Chem. Chem. Phys.* **2016**, *18*, 32560–32569.
- (96) Melcr, J.; Martinez-Seara, H.; Nencini, R.; Kolafa, J.; Jungwirth, P.; Ollila, O. H. S. Accurate Binding of Sodium and Calcium to a POPC Bilayer by Effective Inclusion of Electronic Polarization. *J. Phys. Chem. B* **2018**, *122*, 4546–4557.

- (97) Ollila, O. H. S. CHARMM36 Simulations of POPC Mixed with Cationic Surfactant. 2018; <https://doi.org/10.5281/zenodo.1288297>.
- (98) Dvinskikh, S. V.; Zimmermann, H.; Maliniak, A.; Sandstrom, D. Measurements of Motionally Averaged Heteronuclear Dipolar Couplings in MAS NMR Using R-Type Recoupling. *J. Magn. Reson.* **2004**, *168*, 194–201.
- (99) Browning, J. L.; Seelig, J. Bilayers of Phosphatidylserine: A Deuterium and Phosphorus Nuclear Magnetic Resonance Study. *Biochemistry* **1980**, *19*, 1262–1270.
- (100) Melcr, J. POPC Lipid Membrane, 303K, Charmm36 Force Field, Simulation Files and 200 Ns Trajectory for Gromacs MD Simulation Engine V5.1.2. 2016; <https://doi.org/10.5281/zenodo.153944>.
- (101) Favela-Rosales, F. MD Simulation Trajectory of a Lipid Bilayer: Pure POPC in Water. SLIPIDS, Gromacs 4.6.3. 2016. 2016; <https://doi.org/10.5281/zenodo.166034>.
- (102) Hauser, H.; Shipley, G. G. Interactions of Monovalent Cations with Phosphatidylserine Bilayer Membranes. *Biochemistry* **1983**, *22*, 2171–2178.
- (103) Hauser, H.; Shipley, G. Comparative Structural Aspects of Cation Binding to Phosphatidylserine Bilayers. *Biochim. Biophys. Acta* **1985**, *813*, 343 – 346.
- (104) Mattai, J.; Hauser, H.; Demel, R. A.; Shipley, G. G. Interactions of Metal Ions with Phosphatidylserine Bilayer Membranes: Effect of Hydrocarbon Chain Unsaturation. *Biochemistry* **1989**, *28*, 2322–2330.
- (105) Cevc, G. Membrane Electrostatics. *Biochim. Biophys. Acta* **1990**, *1031*, 311 – 382.
- (106) Nencini, R. Simulation Data for CHARMM36 POPC Bilayer, 100 Lipids/leaflet, 310K, GROMACS 5.1.4. 2018; <https://doi.org/10.5281/zenodo.1198158>.

- (107) Nencini, R. Simulation Data for CHARMM36 POPC Bilayer, 100 Lipids/leaflet, 940 mM NaCl, 310K, GROMACS 5.1.4. 2018; <https://doi.org/10.5281/zenodo.1198454>.
- (108) Nencini, R. Simulation Data for CHARMM36 POPC Bilayer, 100 Lipids/leaflet, 450 mM CaCl₂ ("NB-Fix" Used), 310K, GROMACS 5.1.4. 2018; <https://doi.org/10.5281/zenodo.1198171>.
- (109) Javanainen, M. POPC @ 310K, 450 mM of CaCl₂. Charmm36 with Default Charmm Ions. 2016; <http://dx.doi.org/10.5281/zenodo.51185>.